Anyon-Hubbard model in optical lattices

Julian Felipe Arcila Forero

Physics Department-Sciences Faculty
Universidad Nacional de Colombia
Bogotá, Colombia
2017

Anyon-Hubbard model in optical lattices

Julian Felipe Arcila Forero

For the acquisition of the degree of:
Master of Science in Physics

Advisor:
Jereson Silva Valencia, Ph.D.

Research Field:
Ultracold atoms confined in one-dimensional optical lattice
Research Group:
Correlated Systems group

Physics Department-Sciences Faculty
Universidad Nacional de Colombia
Bogotá, Colombia
2017

To the memory of Don Gonzalo and Doña Helda and my parent's perseverance, love and unconditional support.

Papers and Presentations

During the realization of the present work, the following papers have been published in (or submitted to) international reviews:

- J. Arcila-Forero, R Franco, and J Silva-Valencia, *Emergence of the Mott lobe with $\rho = 1$ for anyons with local three-body interactions*, with referees in Physical Review A (2017)
- J. Arcila-Forero, R Franco, and J Silva-Valencia, *Critical points of the anyon-Hubbard model*, Physical Review A **94**, 013611(2016)
- J. Arcila-Forero, R Franco, and J Silva-Valencia *Density matrix renormalization group study of the Anyon-Hubbard model*, Journal of Physics: Conference Series **687** 012064 (2016)

Different parts of the work were presented in the following national and international events:

- APS March Meeting 2017. New Orlean-Louisiana, United States. March 13-17, 2017. Presentation: *One-dimensional anyons under three-body interactions* - performed by Jereson Silva Valencia, Ph.D.
- School on Interaction of Light with Cold Atoms. International Center for Theoretical Physics-South American Institute for Fundamental Research (ICTP-SAIFR). Sao Paulo, Brazil. January 30-February 10, 2017. Presentation: *Critical points of the anyon-Hubbard model.*
- XVIII International Conference on Recent Progress in Many Body Theories. University at Buffalo. Niagara Falls – NY, United States. August 16-21, 2015. Presentation: *Superfluid to Mott insulator transition of anyons with statistical phase $\pi/4$.*
- 2015 International Symposium on Quantum Fluids and Solids. University at Buffalo. Niagara Falls – NY, United States. August 9-15, 2015. Presentation: *Superfluid to Mott insulator transition of anyons with statistical phase $\pi/4$.*
- Escuela de Física teórica: Teoría cuántica de campos. Universidad del Norte. Barranquilla, Colombia. October 26-30, 2015. Presentation: *Entanglement in the anyon-Hubbard model.*
- Topological Quantum Matter: From Theory to applications. Universidad de los Andes Bogotá, Colombia. May 25-29, 2015. Presentation: *Phase transition of anyons confined in one-dimensional optical lattice.*

- 3rd International Meeting For Researchers In Materials And Plasma Technology. 1 St Symposium on nanoscience and nanotechnology. Universidad Pontificia Bolivariana. Bucaramanga, Colombia. May 4-9, 2015. Presentation: *Density matrix renormalization group study of the Anyon-Hubbard model*

- 2nd workshop on statistical physics. Universidad de los Andes. Bogotá, Colombia. September 22-26, 2014. Presentation: *Anyons in one-dimensional optical lattice.*

Acknowledgements

I thank Professor Silva-Valencia, who designed and directed this project, for his enormous commitment and exceptional ability to guide this research, his interest in my academic growth, and for his valuable lessons about the scientific endeavor and life itself.

I send a special thanks to the Arcila-Forero family for their unconditional support during this research and for their confidence in me during this academic stage — you are one of my greatest motivations. I also thank Adriana Cabrera, who was a very important part of the development of this thesis; thank you for all your love, support and understanding in this period of our lives—we keep making history. To Andrés Hincapie, with whom I shared long afternoons of discussion about this research and the good news of academic life, thanks for our great friendship over these years. Thanks too to Diego Muñoz for his continuous discussions about the implications and possible applications of this research in other physical contexts, but especially for his friendship. Finally, I thank the Correlated Systems Group, directed by professors Roberto Franco and Jereson Silva, who welcomed me and allowed me to do research with them; surely there was no better place to discuss and think about the physics of ultra-cold atoms— I will always be grateful.

I am thankful for the support of DIEB - Universidad Nacional de Colombia and Departamento Administrativo de Ciencia, Tecnología e Innovación (COLCIENCAS) (Grant No. FP44842-057-2015 - *Diagrama de fases de átomos fermiónicos, bosónicos y aniones en redes ópticas*).

Abstract

Anyons can be considered to be a third class of particles with nontrivial exchange statistics that interpolate between fermions and bosons (they do not obey Bose-Einstein or Fermi-Dirac statistics). For two anyons under particle exchange, the wave function acquires a fractional phase $e^{i\theta}$, giving rise to fractional statistics with $0 < \theta < \pi$. We study the properties of a collective of anyons loaded in an one-dimensional optical lattice at a zero temperature. We study a Hubbard model of anyons that takes into account the hopping of the particles along the lattice and the local two-body interaction between them. With the aim to proposing a realistic setup, Keilmann *et al.* introduces an exact mapping between anyons and bosons in one-dimension (the fractional version of the Jordan-Wigner transformation) [1]. We used this exact mapping and we studied the anyon-Hubbard Hamitonian in terms of bosonic operators. Thus, the model is a modified Bose-Hubbard model where the tunneling depends on the local density and the interchange angle ($t \to te^{i\theta n_j}$). The study was performed by means of the density matrix renormalization group (DMRG), which has allowed us to obtain the phase diagram for different values of the statistical angle θ and densities $\rho = N/L$. We observe the gapped (Mott insulator) and gapless (superfluid) phases that characterized the phase diagram and we calculated these phase diagram for higher densities. The phase transition was studied using the block von Neumman entropy, and we were able to observe the superfluid to Mott insulator transition. In particular, we use the estimator proposed by Läuchli and Kollath to determine the critical points, which has enabled us to present the evolution of the critical point with the global density and the statistical angle. On the other hand, when we change the local interaction in the system, anyons interacting via repulsive local three-body interactions, the quantum phase transition is driven by the statistics and the appearence of Mott insulator states, for the system with $\rho = 1$, depends on the anyonic angle. We showed the phases diagram and it was possible to study the influence of the many-body interactions on critical point position.

Keywords: Anyons, one-dimension, optical lattice, -Hubbard model, DMRG, quantum transition, entanglement.

Resumen

Los aniones pueden ser considerados como una tercera categoría de partículas con un una estadística de intercambio no trivial, que interpolan entre fermiones y bosones (no obedecen a las estadísitca de Bose-Einstein ni Fermi-Dirac). Para dos aniones bajo intercambio de partículas, la función de onda adquiere una fase fraccional $e^{i\theta}$, dando lugar a una estadística fraccional con $0 < \theta < \pi$. Nosotros estudiamos la propiedades de una colectivo de aniones cargados en una red óptica unidimensional a temperatura cero. Estudiamos un modelo Hubbard de aniones que tiene en cuenta el salto de las partículas a lo largo de la red y la interacción local de dos cuerpos entre ellas. Con el objetivo de proponer un esquema realístico, Keilmann *et al.* introducen un mapeo exacto entre aniones y bosones en una dimensión (La versión fraccional de la transformación de Jordan-Wigner). Nosotros usamos este mapeo exacto y estudiamos el Hamiltoniano de anyon-Hubbard en términos de operadores bosónicos. Así, el modelo es una modelo de Bose-Hubbard modificado en donde el tunelamiento depende de la densidad y el ángulo de intercambio ($t \to te^{i\theta}$). El estudio se realizó por medio del grupo de renormalización de la matriz densidad (DMRG, por su sigla en inglés), el cual nos permitió obtener los diagramas de fases para diferentes valores del ángulo de la estadística θ y de la densidad $\rho = N/L$. Nosotros observamos una fase con gap (aislante de Mott) y una fase sin gap (superfluida) que caracteriza a los diagramas de fase y calculamos estos diagramas para altas densidades. La transición de fase fue estudiada usando la entropía de bloque de von Neumann y fue posible observar la transición de superfluido a aislante de Mott. En particular, usamos el estimador propuesto por Läuchli y Kollath para determinar los puntos críticos, lo cual nos permitió presentar la evolución de los puntos críticos con la densidad global y con el ángulo de la estadística. Por otra parte, cuando cambiamos la interacción local en el sistema, aniones interactuando por medio de una interacción repulsiva de tres cuerpos. La transición de fase cuántica es manejada por la estadística y la aparición de estados aislantes de Mott, para el sistema con $\rho = 1$, dependen del ángulo aniónico. Nosotros mostramos los diagrmas de fase y fue posible estudiar la influencia de las interacciones de muchos cuerpos sobre la posición del punto crítico.

Palabras Clave: Aniones, una dimensión, redes ópticas, modelo -Hubbard, DMRG, transición cuántica, entrelazamiento .

Contents

List of Figures

Chapter 1

Introduction

One of the most important aspects regarding the nature of indistinguishable particles is the symmetry and anti-symmetry of the wave function under two-particle exchange. Quantum theory shows us that if the wave function is not modified by the exchange of two particles, we have bosons. These particles can occupy the same quantum state and their wave function is symmetrical. Nevertheless, another group of particles exists, the fermions. Under particle exchange, their wave function acquires a -1, this being an anti-symmetrical wave function. Consequently, fermions cannot have the same quantum state when they are together.

In this way, the relevant aspect in the identification of bosons and fermions lies in two-particle exchange. Here, a very interesting question arises regarding the influence that the type of exchange performed on the particles has on the system. In other words, it involves no longer thinking of the exchange of particles as a "mathematical procedure" (index exchange) and instead considering the path, or physical process by which we cause two particles to exchange positions. If a dependency on the type of exchange performed on the two particles existed, the bosons and the fermions could not be the only possible results. Rather, they would be the limit cases (symmetrical and anti-symmetrical). This question was approached by Leinnas and Myrheim [5] who showed that it is possible to find intermediate behaviors when two-dimensional systems are considered. We distance ourselves from what could be the "trivial" case in three dimensions to bring forward an exotic result when two particles are exchange in a low-dimension system (2D). More concretely, it was shown that under certain circumstances, the exchange of two particles results in the appearance of an arbitrary phase factor in the wave function that differs from the case of bosons and fermions. Considering that this exchange results in "any" phase, these particles given the generic name of "anyons." This name was proposed by Wilckzek in 1982 [6].

One way of illustrating this is by considering a pair of identical particles that change their positions along a specific trajectory [7]. In general, the wave function acquires a $e^{i\theta}$ factor. In three dimensions, two successive exchanges result in an identity transformation. Thus, a

single topological path exists to permute the two particles. In that case, θ has a value of 0 or π (bosons and fermions, respectively). However, in two dimensions, the double exchange corresponds to one particle completing a complete rotation around the other. This movement is not topologically trivial. In that case, it is possible to find different exchange paths that are not topologically equivalent [8]. Then, a $e^{i\theta}$ factor appears with θ values between $(0, \pi)$, giving way to a new statistic that is induced with one of the possible θ values. Furthermore, the anyons studied by Wilczeck [6] appear in the context of electrodynamics, an interaction between electric charges and vortices that carry a magnetic flux in two dimensions. Separately, each type of particle is a boson, but when the electric charge revolves around the vortex, it acquires a non-trivial exchange phase [7] leading to anyonic states.

Today, among the most important evidence of the existence of anyons in nature is to be found when a gas of electrons is enclosed over a thin film under the action of a very strong magnetic field and at a low enough temperature to result in the fractional quantum Hall effect (observed experimentally) [9, 10]. The excitations of this system exhibit anyonic statistics and possess well-defined topological orders [8].

D. Haldane, carried out an important study on the possibility to find this type of excitations in other dimensions different to the two-dimensional case [11]. First of all, he delimited the presence of anyons to a patch of the condensed matter. More precisely, the anyons would be topological excitations of a state of condensed matter. These particles can be recognized by the presence of states with an unusual or variable number of particle states that are not explained by the simple interaction of the components of the system [11]. It given rise to a new statistic, this statistics is known as a *fractional statistics*. Furthermore, he conluded that the anyons statistics does not depend on the dimension of the system. This opened the possibility of applications beyond the two-dimensional context, making the concept of anyons important in arbitrary dimensions [11].

Without two-dimensional constraint, different efforts have been made to study anyons from the experimental and theoretical perspective, giving rise to the discovery of important physical properties and discussion of some applications, for example in quantum information theory, in the study of the topological states of condensed matter, in the fractional quantum Hall effect. Another application that has become quite relevant in recent years is the use of anyons in quantum computing, given its characteristics of fault tolerance [7]. Nevertheless, the topic of fractional statistics continues to be a field with much potential since it has not been widely studied. Furthermore, the study of anyons continues to be considered as exotic as the very nature of these particles.

On the other hand, we want to highlight the current importance of optical lattices in the study of strongly correlated systems. Today, they are used as simulators of systems of con-

densed matter because of the possibility of controlling in an extremely precise way the parameters on which a Hamiltonian depends without the normal uncertainty that comes with experiments on materials. This offers, for example, to the fascinating possibility of observing quantum phase transitions in gasses of ultra-cold atoms, of studying the dynamics of a gas on the optical lattice, and, among other things, of simulating complex structures of real materials in optical lattices while restricting the spatial dimensions, which is an excellent bridge between materials-based condensed matter physics and cold atoms.

Keilmann and collaborators in 2011 [1] proposed the anyon-Hubbard model, which describes a system of anyons on a one-dimensional optical lattice in the context of ultra-cold atoms at zero temperature. The model considers two terms: the first is associated with particle's possibility of moving between the sites of the lattice (one site at a time), while the second terms is related to the particle's interaction in the same site due to Coulomb repulsion. For study this Hamiltonian they introduced an exact mapping between bosons and anyons, by means of a fractional Jordan-Wigner transformation. The regular Jordan-Wigner transformation was proposed for one-dimensional lattice models and it is a map beetwen spin operators onto operators that obey fermionic commutations relations. Using the transformation is possible to exactly solve one-dimensional problems and to obtain the set of energies in the fermionic base [12]. After using the fractional version of Jordan-Wigner transformation, the anyon-Hubbard model results in a modified Bose-Hubbard model where the tunneling depends on the local density and the interchange angle θ. The use of this mapping allows the experimental creation of anyons using bosons with occupation-dependent hopping amplitudes [1].

From the theoretical point of view, an interesting aspect of Keilmann *et al.* study [1] is the development of a phase diagram in which the influence of the anionization of the gas can be seen (increase in the statistical angle). To start, they demonstrated that the gas has two quantum phases. First, a superfluid phase characterized by the absence of a gap in the thermodynamic limit. In this phase, the particles are dispersed over the entire lattice and an overlapping of the wave functions occurs. Second, a Mott-insulator phase appears, characterized by the presence of a gap in the thermodynamic limit and an equal occupation of particles in every site of the lattice. Here, a non-coherent phase occurs over the entire optical lattice. In the Fig. **1-1**, the phase diagram obtained by Keilmann for density $\rho = 1$ can be observed [1]; there, the phase transition between a Mott-insulator phase and a superfluid can be seen as the tunneling of the particles increases. An aspect of great interest is the expansion of the Mott lobe in both directions when the statistical angle is increased [1]. The Mott-insulator state is favored in the system. Furthermore, in the inset of the Fig. **1-1**, the evolution of the critical points, calculated with the gap closure, is shown.

For the improve the proposal for the realization of Keilmann's anyon-Hubbard model. Greschner and Santos proposed an experimental scheme with a two-body hard constraint which

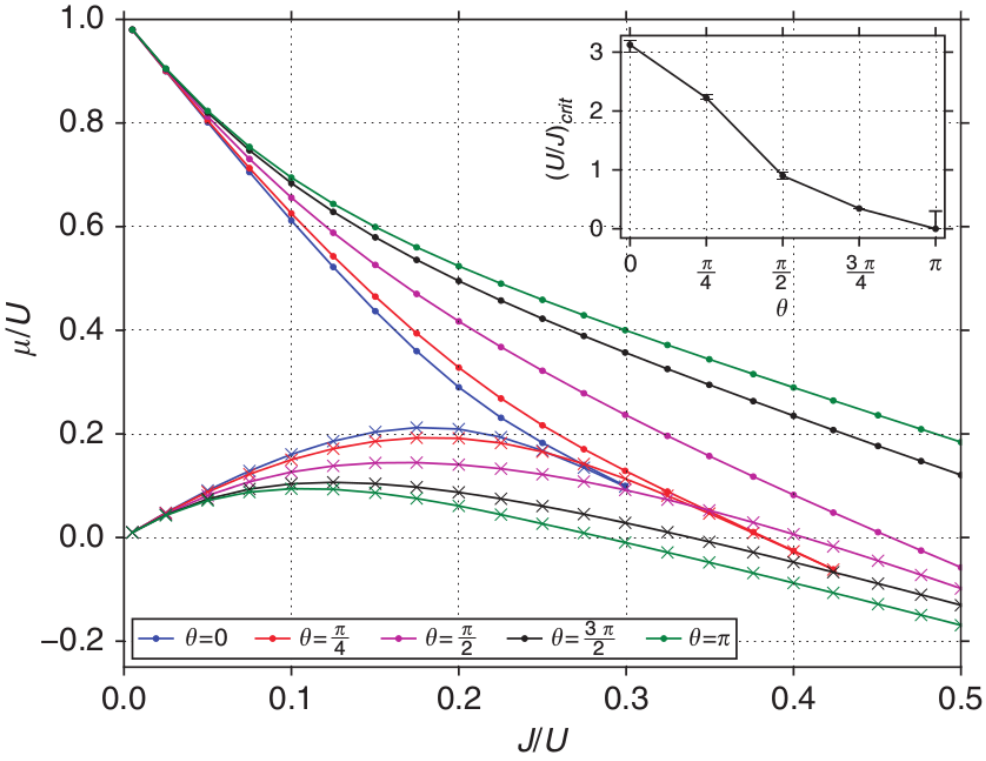

Figure 1-1: Phase diagram of the anyonized gas. Statistically induced phase transitions and anyons in 1D optical lattices [1].

results in a far richer physics for the model, and the phase diagram includes exotic quantum phases [2]. Among others, an interesting result is presented in this work, the equation of state ($\rho = \rho(\mu)$) for anyons with $\theta = \pi$ without local interactions, this anyon's system present three quantum phases, superfluid, paired phase and Mott-Insulator [2].

However, the bosonic mapping is not the only one. Hao *et al.* studied a hard-core anyonic Hamiltonian with anyons that can be mapped onto the non-interacting fermionic system, the Hamiltonian is rewritten in terms of operators for spinless fermions. They investigated the ground state [13] and dynamical [14] properties of anyons confined in one-dimensional optical lattices with a weak harmonic trap using an exact numerical method based on a generalized Jordan-Wigner transformation.

Considering all the previous arguments, we are interested in the study of the anyon-Hubbard model and, particularly, the study of the quantum phase transitions that take place in one dimension. To start, there is a very interesting question that should be considered: what is the influence of the increase in the density of the system on the position of the critical point and the type of quantum phases present in the system?. To this end, we will obtain the correct phase diagrams to be able to make conclusions about this dependency and we

will verify if the size and/or the shape of the regions is affected. Initially, we will focus on the case of statistics with $\theta = \pi/4$ and thereby corroborate the asymmetry present in the phase diagram of the mean field or refute the hypothesis of the approximate calculation by Keilmann *et al.* [1]. Later, we will carry out a study with other statistical values.

On the other hand, the tools of quantum information theory have been used successfully to study the critical behavior of different models of condensed matter physics [15]. Some tools can be used to characterize the quantum phases present in systems of condensed matter. They even allow the estimation of the border or critical point that separates one region from another (or others) [16]. For example, measures of the entanglement, such as fidelity, von Neumann entropy, purity, and negativity, among other have been useful. For the Bose-Hubbard, the von Neumann block entropy has been used to observe the critical and non-critical behavior in the system [15,17,18]. In 2015, Islam and collaborators performed direct measurements of quantum purity, Rényi entanglement entropy, and mutual information in a Bose-Hubbard system [19]. Thus, the theoretical predictions can be proved experimentally and reinforced that the relationship between entanglement and quantum phase transitions are an important topic at present. In this work, we will use the von Neumman block entropy to study the ground state of the anyon Hamiltonian.

Specifically, We wish to answer the question: is it possible to observe the critical (superfluid states) and non-critical (Mott-insulator phase) nature of the system of anyons by way of von Neumann block entropy? In this way, we could estimate the critical point using the estimator proposed by Läuchli and Kollath, which is written in terms of this entropy [17]. Moreover, an interesting question arises that is associated with the evolution of the critical points as we increase the density of the system and the possibility of obtaining a functional dependence of this evolution for a certain statistical value. Likewise, we can study the evolution of the critical points with the angle, setting one density in particular. This question will be approached, and we would like to highlight the fact that no previous studies exist regarding the more precise estimation of the critical points of the anyon-Hubbard model beyond the gap closure.

Another aspect that has not been reported and that complements this study is the discussion regarding the way in which the quantum phase transition occurs; that is, to answer the question: What is the type of transition that occurs in the system? This permits a determination of the kind of universality that the model is part of, at least for a certain value of fractional statistics. This study can be done for various densities.

Finally, we are interested in studying an anyon model whose local interaction has been modified, the particles interaction via repulsive local three-body interactions. The main motivations are the recent works, in the regime in which dominant interactions are those involving many bodies [20]. Also, the exotic quantum phases that apears when is consider many-body

terms in Hamiltonians [21–23]. Buchler *et al.* showed that polar molecules in optical lattices can be tuned to a regime where the three-body interactions are dominant [23]. Moreover, Johnson *et al.* showed that there are effective three- and higher-body interactions generated by the two-body collisions of atoms [24]. On the other hand, evidence was found of multi-body interactions using an interferometric technique for ^{87}Rb atoms confined in an optical lattice [25]; the measurements of multi-body interaction energies provides crucial input for the comparison of optical-lattice quantum simulators with many-body quantum theory [25]. Recently, was present a simple, experimentally realizable method to make coherent three-body interactions dominate the physics of an ultracold lattice gas. This scheme allows to reduce or turn off two-body interactions in a rotating frame, promoting three-body interactions [20].

In this case, it's important to consider two fundamental aspects: first, that interactions involving many bodies modify the phase diagrams and second, that the localization of particles depends on statistics value that induces the presence of a fractional phase in the Hamiltonian [1, 26]. These two ingredients in the model lead to the appearance of interesting effects that have not been reported previously.

For all calculations, we used the density matrix renormalization group (DMRG) method. This method was developed by S. White in 1992 [27] and has become a powerful numerical method that can be applied to low-dimensional strongly-correlated fermionic and bosonic systems. Its field of applicability has now been extended beyond condensed matter, and it is successfully used in statistical mechanics and high-energy physics. The DMRG allows for a systematic truncation of the Hilbert space by keeping the most probable states that describe a wave function [28].

We performed a numerical study of anyons in one-dimension and we found the quantum phases of the anyon-Hubbard model with two- and three-body interactions. We computed the chemical potential at the thermodynamic limit and found the phase diagrams, which could be useful for experimentalists and the stimulation of future studies.

Chapter 2

Anyons and the anyon-Hubbard model

2.1. Previous studies in one dimension

Commonly, the particles in quantum theory are classified in two types, bosons and fermions, associated with the particle exchange. For two bosons the wavefunction remains invariant under particle exchange, whereas the exchange of two fermions leads due to the Pauli principle to a phase factor -1 in the wavefunction. Physicists have proposed a third class of particles with nontrivial exchange statistics, anyons, particles carrying fractional statistics that interpolate between bosons and fermions [5,6,11]. For two anyons under particle exchange, the wave function acquires a fractional phase $e^{i\theta}$, giving rise to fractional statistics with $0 < \theta < \pi$. Greater interest in the study of anyons emerged when the fractional quantum Hall effect, observed experimentally, had a natural explanation in terms of anyons [9, 10]. Another discovery that reinforced this interest was evidence of superconductor anyon gas [29,30]. Anyons are very important in numerous studies related to the fractional quantum Hall effect [31,32], condensed matter physics, and topological quantum computation [7,33,34]. The study of anyons was restricted for many years to two-dimensional systems. However, with Haldane's definition of fractional statistics, it was generalized to arbitrary dimensions [11].

One-dimensional (1D) anyons have been studied from different theoretical approaches. Kundu obtained the exact solution of the one-dimensional anyon gas using the generalized coordinate Bethe ansatz method and found the generalized commutation relations for anyons [35]. Furthermore, Batchelor *et al.* showed that the low energies, the dispersion relations, and the generalized exclusion statistics depend on both the anyonic statistical angle and the dynamical interaction parameters in a 1D anyon gas [36]. Alternatively, in tight waveguides, the Fermi-Bose mapping method for one-dimensional Bose and Fermi gases was generalized to an anyon-fermion mapping and applied in order to obtain exact solutions of several models of ultracold gases with anyonic exchange symmetry [37]. In 2007, Calabrese and Mintchev

studied the correlation functions of the 1D anyonic gapless systems in the low-momentum regime [38]. Interesting features appear, including universal oscillating terms with frequency proportional to the statistical parameter and beating effects close to the fermion points. Later, Vitoriano and Coutinho-Filho [39] studied the ground state and low-temperature properties of an integrable Hubbard model with bond-charge interaction, finding that the model displays fractional statistical properties. Remarkably, one-dimensional anyons can be realized as low-energy excitations of the Hubbard model of fermions with correlated hopping processes. On the other hand, Hao *et al.* investigated the ground state [13] and dynamical [14] properties of anyons confined in one-dimensional optical lattices with a weak harmonic trap using an exact numerical method based on a generalized Jordan-Wigner transformation. Also, two-component mixtures of anyons under an external trap were considered by Zinner [40] and the correlation functions of one-dimensional hard-core anyons were calculated by Patu [41].

Note that various experimental proposals for the creation fractional statistics have been made. Rotating Bose-Einstein condensates have been used to create anyons [42], and the results can be understood in terms of the fractional quantum Hall effect for bosons [43]. This system offers the formation of particles exhibiting fractional statistics with a well-controlled setup that can allow experimentalists to test their fractional statistics. Later on, Duan and colleagues described a general technique for controlling many-body spin Hamiltonians using ultracold atoms, and they showed how to implement an exactly-solvable spin Hamiltonian that supports Abelian and non-Abelian anyonic excitations with exotic fractional statistics [44]. On the other hand, it is possible to use an atomic spin lattice in optical cavities for the direct measurement of anyonic statistics [45] or trapped atoms in an optical lattice in order to create anyons in topological lattice models. These types of schemes allow the creation of topologically ordered states and detect their statistics [46]. Alternatively, a suggestion has been made for creating anyons on a 1D lattice based on light propagation in an engineered array of optical waveguides. This photonic setup enables us to see the impact of the statistical exchange phase θ on the correlated tunneling dynamics [47]. Furthermore, the possibility of realizing the bosonic fractional quantum Hall effect in ultracold atomic systems has been shown, suggesting a new route to producing and manipulating anyons [48].

Using optical lattice have been made proposals for using ultracold bosons to produce anyons. Keilmann *et al.* propose a realistic setup for create anyons with bosons with correlated tunelling in a 1D optical lattice [1]. From the theoretical point of view, They found, among other things, the phase diagram at zero-temperature with density $\rho = 1$ using the density matrix renormalization group, and concluded that the anyons in 1D display insulator and superfluid phases. In addition, they presented the mean-field solution for the Mott-superfluid transition for different angles and a comparison with the bosonic case, where it is possible to see the expansion of the Mott lobes with the statistical angle [1]. Later on, the ground-state

properties of anyons in a one-dimensional lattice were analyzed by Tang *et al.* [49] using the Hamiltonian proposed by Keilmann *et al.* [1], and they obtained that anyons have an asymmetric quasi-momentum distribution, where the peak position depends on both the fractional phase and the particle number density. In the same way, the momentum distributions and the effects of the statistical angle on the correlations were analyzed using the density matrix renormalization group and mean field methods by Zhang *et al.*, finding that the statistical angle could modulate the beat length of the correlations [50].

Other study concentrated the attention in the statistically induced quantum phase transition between Mott-insulator and superfluid phases, and the stimation of the critical points using quantum information tools [26]. Also, some works focused on the study of the one-body reduced density matrix of a system of N one-dimensional impenetrable anyons trapped by a harmonic potential which provides a theoretical tool for future cold atom experiments [51], the systematically study the pseudo-anyon-Hubbard model on a one-dimensional lattice without the presence of a three-body hardcore constraint [52] and the numerical demonstration of the existence of a nontrivial topological Haldane phase for anyons in the one-dimensional extended Hubbard model with a mean density of one particle per site [53]. Ejima *et al.* apply perturbation theory for study strongly repulsive anyons in one-dimension. They found antalytic expressions valid for any fractional phase θ of anyons thinking in future experiments. Also, they calculate the ground-state energy and the distribution functions using density matrix renormalization gruop technique [54].

2.2. Anyon-Hubbard Hamiltonian

For anyons in one-dimension, $a_j^\dagger$ and a_j are the creation and annihilation operators at the site j, respectively. These operators satisfying (are definied by) the anyonic commutation relations

$$\begin{aligned} a_j a_k^\dagger - e^{-i\theta sgn(j-k)} a_k^\dagger a_j &= \delta_{jk}, \\ a_j a_k - e^{i\theta sgn(j-k)} a_k a_j &= 0, \end{aligned} \tag{2-1}$$

where θ denotes the statistical phase, and the sign function (multistep function) is $sgn(j-k) = \pm 1$ for $j > k$ and $j < k$, and $= 0$ for $j = k$. Two particles on the same site reproduce the ordinary bosonic commutations relations.

The anyon-Hubbard model takes into account the hopping of the anyons along the lattice

and the local two-body interaction between them [1], and its Hamiltonian is given by

$$H = -t\sum_{j}^{L-1}\left(a_j^\dagger a_{j+1} + h.c\right) + \frac{U}{2}\sum_{j}^{L} n_j(n_j-1), \tag{2-2}$$

where $t > 0$ is the tunneling amplitude connecting two neighboring sites, U is the on-site interaction, L is the length of the lattice, n_j is the number operator.

With the aim to propose a realistic setup was introduced an exact mapping between anyons and bosons in one-dimension. Keilmann *et al.* define the fractional version of a Jordan-Wigner transformation [1]

$$a_j = b_j\, exp\left(i\theta\sum_{i=1}^{j-1} n_i\right), \tag{2-3}$$

where the operator b_j describes spinless bosons, which satisfy $[b_j, b_i^\dagger] = \delta_{ji}$ and $[b_j, b_i] = 0$. The number operator is defined by $n_i = a_i^\dagger a_i = b_i^\dagger b_i$.

In the following we prove that the operator a, write in terms of bosonic operators, defined by the relation (2-3), obey the anyonic commutation relations (2-1).

For the case $i < j$ the product of anyonic operators using the fractional Jordan–Wigner mapping results:

$$\begin{aligned} a_i a_j^\dagger &= b_i e^{-i\theta\sum_{i\le k<j} n_k} b_j^\dagger \\ &= e^{-i\theta\sum_{i<k<j} n_k} b_i b_j^\dagger e^{-i\theta n_i}, \\ f(\theta)a_j^\dagger a_i &= e^{-i\theta\sum_{i<k<j} n_k} e^{-i\theta n_i} f(\theta) b_j^\dagger b_i \\ &= e^{-i\theta\sum_{i<k<j} n_k} e^{-i\theta(n_i+1)} f(\theta) b_j^\dagger b_i, \end{aligned} \tag{2-4}$$

we consider that $f(\theta) = e^{i\theta sgn(i-j)}$ and we use that $f(\theta) = e^{-i\theta}$, as $i < j$ was assumed.

We evaluate the first part of equation (2-1):

$$\begin{aligned} a_i a_j^\dagger - f(\theta)a_j^\dagger a_i &= e^{-i\theta\sum_{i<k<j} n_k}(b_i b_j^\dagger e^{-i\theta n_i} - e^{-i\theta(n_i+1)} b_j^\dagger b_i) \\ &= e^{-i\theta\sum_{i<k<j} n_k} e^{-i\theta(n_i+1)}[b_i, b_j^\dagger] \\ &= 0. \end{aligned} \tag{2-5}$$

Then, it is complete the proof for the commutation relations of anyons for the case $i < j$. The proof for the case $i > j$ is analogue. For the case $i = j$, is important to note that $a_i^\dagger a_i = b_i^\dagger b_i$ y $f(\theta) = 1$ [1].

After using the anyon-boson mapping (2-3), the anyon-Hubbard Hamitonian is given in terms of bosonic operators thus:

$$H = -t\sum_{j}^{L-1}\left(b_j^\dagger b_{j+1}e^{i\theta n_j} + h.c.\right) + \frac{U}{2}\sum_{j}^{L} n_j(n_j-1). \tag{2-6}$$

Note that the above Hamiltonian describes bosons with an occupation-dependent amplitude $te^{i\theta n_j}$ for hopping processes from right to left ($j+1 \to j$). If the target site j is unoccupied, the hopping amplitude is simply t. If it is occupied by one boson, the amplitude reads $te^{i\theta}$, for two bosons $te^{i2\theta}$, and so on.

In the following is presented a simple example of Hamiltonian's block for two sites and a sector with four particles. The competition of these three parameters (t, U y θ) determine the quantum state.

$$\begin{array}{c} \\ \langle 2,2| \\ \langle 1,3| \\ \langle 3,1| \\ \langle 0,4| \\ \langle 4,0| \end{array} \begin{array}{c} \begin{array}{ccccc} |2,2\rangle & |1,3\rangle & |3,1\rangle & |0,4\rangle & |4,0\rangle \end{array} \\ \begin{pmatrix} 2U & -\sqrt{6}te^{i\theta} & -\sqrt{6}te^{-i2\theta} & & \\ -\sqrt{6}te^{-i\theta} & 3U & & -2t & \\ -\sqrt{6}te^{i2\theta} & & 3U & & -2te^{-i3\theta} \\ & -2t & & 6U & \\ & & -2te^{i3\theta} & & 6U \end{pmatrix} \end{array}$$

2.2.1. Mean-field calculation

In the following, the mean-field solution performed by Keilmann *et al.* is presented [1]. The anyon-Hubbard Hamiltonian with an additional term, the chemical potential, is given by:

$$H = \sum_j \left[\frac{1}{2}n_j(n_j-1) - \mu n_j - t(c_j^\dagger b_{j+1} + b_{j+1}^\dagger c_j)\right] \tag{2-7}$$

The scale of energy is $U = 1$. Where c_j is defined by $c_j = e^{-i\theta n_j}b_j$.

If the hopping is removed ($t = 0$), all the sites of the lattice are independent and the ground state is of the Gutzwiller type

$$|\Psi_0\rangle = |\Psi\rangle^{\otimes L}, \qquad |\Psi\rangle = \sum_{\rho=0}^{\infty} c_\rho \frac{(b^\dagger)^\rho}{\sqrt{\rho!}}|0\rangle, \tag{2-8}$$

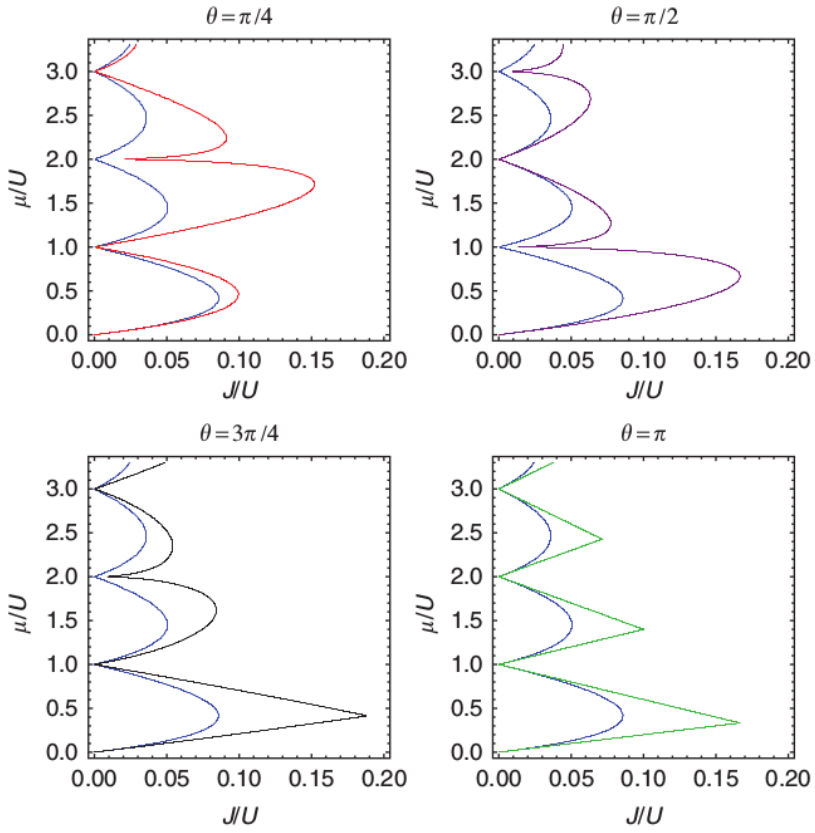

Figure 2-1: Phase diagram from mean field solution for the Mott-superfluid transition for anyons in one-dimension. The blue curve corresponds to bosonic case. Taken from [1].

where $\rho = \frac{N}{L}$ the density of the system. The gaps for adding and substracting one particle are, respectively

$$\epsilon(\rho+1) - \epsilon(\rho) = \rho - \mu, \qquad \epsilon(\rho-1) - \epsilon(\rho) = -(\rho-1) + \mu. \tag{2-9}$$

In contrast, the local energies are $\epsilon\rho = 1/2\rho(\rho-1) - \mu\rho$. In this case, the ground state has ρ particles in the interval $\mu_-^{(\rho)} < \mu < \mu_+^{(\rho)}$, with $\mu_-^{(\rho)} = \rho - 1$ and $\mu_+^{(\rho)} = \rho$.

The mean-field approximation is obtained by decoupling the hopping term as

$$c_j^\dagger b_{j+1} \approx -\alpha_2^* \alpha_1 + \alpha_2^* b_{j+1} + \alpha_1 c_j^\dagger, \tag{2-10}$$

where the order parameters are $\alpha_1 = \langle b_j \rangle$ and $\alpha_2 = \langle c_j \rangle$. The Hamiltonian (2-7) is rewrite in terms of α_1 and α_2,

$$H = \sum_j H_j + Lt(\alpha_2^* \alpha_1 + \alpha_1^* \alpha_2) \tag{2-11}$$

with H_j,

$$H_j = \frac{1}{2} n_j(n_j - 1) - \mu n_j - t \sum_j (\alpha_2 b_j^\dagger + \alpha_2^* b_j + \alpha_1 c_j^\dagger + \alpha_1^* c_j).$$

The parameters α_1 y α_2 are not independent as they are both vanishing or non vanishing at the same time. In this case, the trivial solution with $\alpha_1 = \alpha_2 = 0$, which corresponds to the Mott-insulator phase. The self-consistent relation defines a map $\alpha_l = \Lambda_{ll'}\alpha_{l'}$. If we have $|\alpha_l| << 1$, the term of transport (kinetic term)can be development for perturbatively theory. For the first perturbative order, the wavefunction can be rewritten as $|\psi\rangle = \left|\psi^{(0)}\right\rangle + \left|\psi^{(1)}\right\rangle$, with $\left|\psi^{(0)}\right\rangle = |\rho\rangle$ and

$$\begin{aligned} \left|\psi^{(1)}\right\rangle &= -t \sum_{\rho'} \frac{\langle\rho'| \alpha_2 b_j^\dagger + \alpha_2^* b_j + \alpha_1 c_j^\dagger + \alpha_1^* c_j |\rho\rangle}{\epsilon(\rho) - \epsilon(\rho')} |\rho'\rangle \\ &= t \frac{\sqrt{\rho}(\alpha_2^* + \alpha_1^* e^{-i\theta(\rho-1)})}{\mu - \rho + 1} |\rho - 1\rangle + t \frac{\sqrt{\rho+1}(\alpha_2 + \alpha_1 e^{i\theta\rho})}{\rho - \mu} |\rho + 1\rangle . \end{aligned} \tag{2-12}$$

It is possible to use the self-consistency relations for obtained the next expressions, $\alpha_1 = \langle\psi| b_j |\psi\rangle$ and $\alpha_2 = \langle\psi| c_j |\psi\rangle$, using (2-12) we obtained:

$$\frac{\alpha_1}{t} = \frac{\rho(\alpha_2 + \alpha_1 e^{i\theta(\rho-1)})}{\mu - \rho + 1} + \frac{(\rho+1)(\alpha_2 + \alpha_1 e^{i\theta\rho})}{\rho - \mu}, \tag{2-13}$$

$$\frac{\alpha_2}{t} = \frac{\rho(\alpha_2 e^{-i\theta(\rho-1)} + \alpha_1)}{\mu - \rho + 1} + \frac{(\rho+1)(\alpha_2 e^{-i\theta\rho} + \alpha_1)}{\rho - \mu}. \tag{2-14}$$

In this case, the matrix Λ is

$$\Lambda = t \begin{pmatrix} f(\theta) & A \\ A & f(-\theta) \end{pmatrix}$$

where $f(\theta) = e^{i\theta\rho}[A + (e^{-i\theta} - 1)B]$, the value of constants are

$$A = \frac{\mu + 1}{(\mu - [\mu])([\mu] - \mu + 1)}, \qquad B = \frac{[\mu] + 1}{\mu - [\mu]}.$$

Since every lobe is labelled by $\rho = [\mu] + 1$. The eigenvalues of Λ are given by

$$\lambda_\pm = \frac{t}{2}[f(\theta) + f(-\theta) \pm \sqrt{4A^2 + (f(\theta) - f(-\theta))^2}] \tag{2-15}$$

The Figure **2-1** shows the Mott lobes calculated with the equation (2-15) for different angles and a comparison with the bosonic case, where it is possible to see the reduction of the lobes

with the increases of the density for $\theta = \pi/2, 3\pi/4$ and π. However, for the angle $\theta = \pi/4$ the results shows, an interesting prediction, an odd-even asymmetry between the lobes [1].

2.3. Experimental setup for anyons in one-dimensional optical lattice

In the last years, various experimental proposals for the creation, detection, and manipulation of anyons have been made. We would especially like point out that several proposals for using ultracold bosons to produce anyons in an optical lattice. In particular, Keilmann *et al.* introduced the anyon-Hubbard model, which is equivalent to a modified Bose-Hubbard model in which the bosonic hopping depends on the local density. This is an exact mapping between anyons and bosons in one dimension. They propose a realistic setup for demonstrating an interacting gas of anyons using Raman-assisted hopping in a 1D optical lattice [1]. The statistical angle can thus be controlled *in situ* by modifying the relative phase of external driving fields [1]. In 2015, Greschner and Santos proposed an experimental scheme to improve the proposal for the realization of Keilmann *et al.* This scheme allows as well for an exact realization of the two-body hard constraint (*i.e.* $(b_j^\dagger)^3 = 0$) and controllable effective interactions without the need for Feshbach resonances. They show that the interplay of anyonic statistics, two-body hard constraint, and controllable interactions results in a far richer physics for the model, and the phase diagram includes a pair-superfluid, a dimer, and an exotic partially-paired phase [2]. In addition, the past year, a simple scheme for realizing the physics of 1D anyons with ultracold bosonic atoms in an optical lattice has been elaborated. It relies on lattice-shaking-induced resonant tunneling against potential off-sets created by a combination of a lattice tilt and strong on-site interactions. No lasers in addition to those used for the creation of the optical lattice are required [3]. In the following we present these three experimental proposals.

2.3.1. Assisted Raman tunnelling

In this proposal, the key for the realization of fractional statistics is to induce a kinetic term with a phase shift, which depends on the occupation of the left-hand site j, the dependence with the left-site is possible to see in the correlated tunelling, which depend on n_j, namely, $t(b_j^\dagger b_{j+1} e^{i\theta n_j} + e^{-i\theta n_j} b_{j+1}^\dagger b_j)$. To distinguish between different local occupational states, it is require a non-zero on-site interaction U. For assisted tunelling scheme the optical lattice is tilted, with an energy offset Δ between neighbouring sites (Fig **2-2**). The occupational states are couple to an excited state $|e\rangle$ via four external driving fields. According to Fig **2-2**, singly and doubly occupied states are coupled by fields 2 and 1 in the left site and by 3 and 4 in the right site, respectively. This assisted Raman tunnelling can selectively address hopping

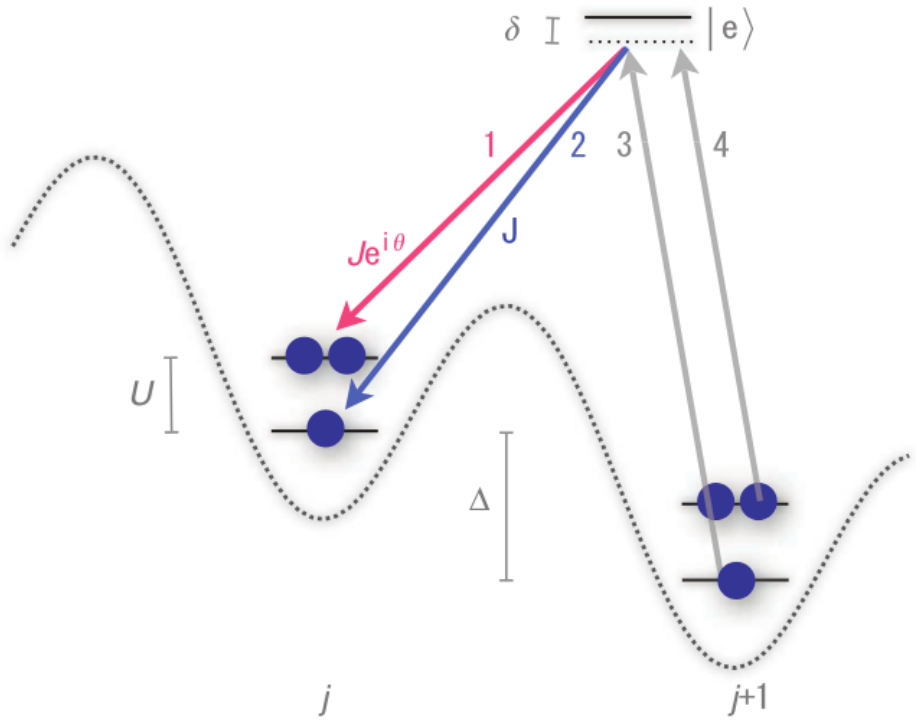

Figure 2-2: Schematic of the experimental proposal. Here, J corresponds to tunneling amplitude hopping parameter. Taken from [1].

processes connecting different occupational states and induce a relative phase, realizing a fully tuneable particle exchange statistics angle θ [1].

For the experimental setup is required two lattices, in the case of ^{87}Rb, one lattice has atoms in the $F = 1$, $m_f = -1$ hyperfine state that corresponds to ground state. The excited state $|e\rangle$ is created with a second lattice, trapping atoms in the $F = 1$, $m_f = 0$ hyperfine state [1]. This setup offer the possibility of external drives held in the radio-frecuency regime which is the same order of magnitude as the system energy scales. Finally, for satisfied the conditional tunneling the next relations should be imposed [1]

$$\begin{aligned} t_{23} = t_{34} = t, \\ t_{13} = t_{14} = te^{i\theta}. \end{aligned} \tag{2-16}$$

2.3.2. Assisted Raman tunnelling + Two-body hard-core constraint

This proposal present a possible improve of the Keilmann *et al.* experimental realization. Greschner and Santos consider atoms (bosons or fermions), with states $|A\rangle$ and $|B\rangle$ in one-dimensional lattice, which is tilted and it not have direct hopping. The authors choice the

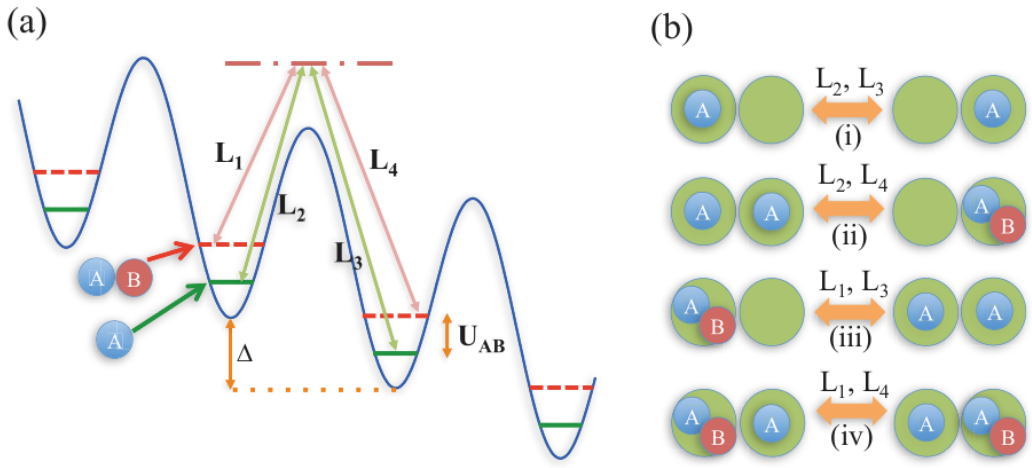

(a) Raman scheme proposed for the realization of the AHM
(b) Raman assisted hops (i)–(iv) discussed in the text.

Figure 2-3: Raman-assisted hopping with two-body hard-core constraint. Taken from [2].

states, $|A\rangle = |F = 1, m_F = -1\rangle$ and $|B\rangle = |F = 2, m_F = -2\rangle$ for the case of ^{87}Rb. The two states are coupled for the lasers L_1 and L_4 with linear polarization and coupled for other two lasers, L_2 and L_3 with circular polarization. The hoppig processes are depicted in Fig **2-3**.

These lasers L_k with frecuencies ω_k induce the Raman-assisted hops. The conditions on the parameters for the coupling nearest sites are:

$$\begin{array}{llll} (A,0) \to (0,A) & L_2 \ and \ L_3 & \omega_2 - \omega_3 = -\Delta, \\ (A,A) \to (0,AB) & L_2 \ and \ L_4 & \omega_2 - \omega_4 = -\Delta + U_{AB} + U, \\ (AB,0) \to (A,A) & L_1 \ and \ L_3 & \omega_1 - \omega_3 = -\Delta - U_{AB}, \\ (AB,A) \to (A,AB) & L_1 \ and \ L_4 & \omega_1 - \omega_4 = -\Delta. \end{array} \tag{2-17}$$

This is the conditional hopping with Raman-assisted tunneling processes for reproduce the anyon-Hubbard model experimentally [2].

2.3.3. Floquet realization

The aim of Sträter and co-workers is to make an experimental setup for anyons in one-dimension without additional laser for the creation of the optical lattice [3]. For the realization of correlated hopping, they consider bosons in a tilted periodically forced lattice which is associated with the following Hamiltonian

$$\hat{H} = \sum_j \left(-t' \left[b_j^\dagger b_{j-1} + h.c \right] + \frac{U'}{2} n_j(n_j - 1) + V_j n_j + [\Delta + F(t)] j n_j \right), \tag{2-18}$$

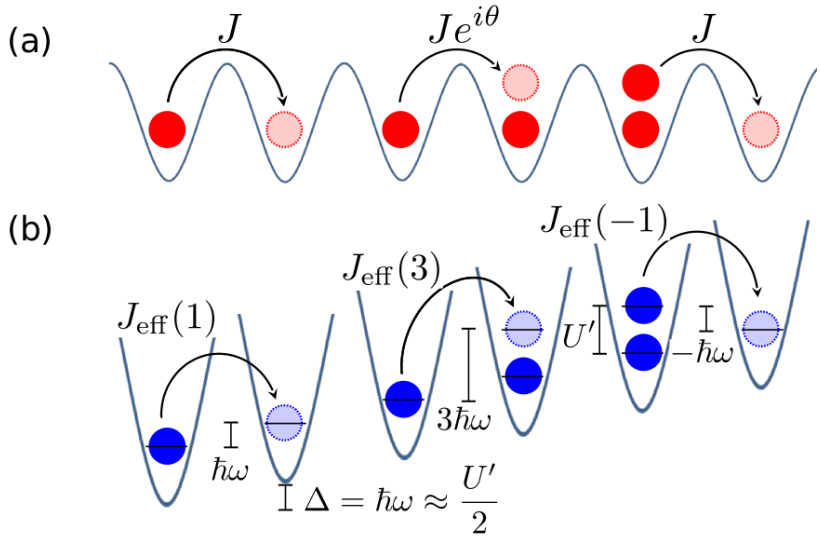

Figure 2-4: Tilted lattice with strong on-site interactions, it depict processes for number-dependent tunneling. Taken from [3].

where Δ characterizes the potential tilt, V_j is related with a weak additional on-site potentials, and $F(t) = F(t+T)$ incorporates a homogeneous time-periodic potential.

The setup requires the next resonance and high frecuency conditions, respectively (Fig. **2-4**):

$$\Delta = \hbar\omega, \qquad U' = 2\hbar\omega, \tag{2-19}$$

$$J', |U|, |V_j - V_{j-1}| \ll \hbar\omega. \tag{2-20}$$

Considering the above conditions, the dominant on-site interaction is given by

$$H_0 = \hbar\omega \sum_j [n_j(n_j - 1) + jn_j], \tag{2-21}$$

then the tunneling is energetically suppresed. Using the time-periodic unitary operator, for applying the Floquet theory in the leading order of a high-frequency approximation is possible to obtain an effective time-independent Hamiltonian,

$$H_{eff} = -\sum_j \left(b_j^\dagger b_{j-1} J_{eff}(\nu_{j,j-1}) + h.c. \right) + \sum_j \left(\frac{U}{2} n_j(n_j - 1) + V_j n_j \right), \tag{2-22}$$

with $\nu_{j,j-1} = 2(n_j - n_{j-1}) + 3 = \pm\hbar\omega, \pm 3\hbar\omega, \ldots$. The correlated tunneling is given by,

$$J_{eff}(\nu) = \frac{J'}{T} \int_0^T exp(i\omega t\nu - i\chi(t))\ dt. \tag{2-23}$$

For the realization of the anyon-Hubbard model, the tunneling elements, $J_{eff}(\nu)$ should reproduce the tunneling dependent of the local density to the original anyon-Hubbard model.

On the other hand, in (2-23), χ satisfies the next relation, $\dot{\chi} = -F(t)/\hbar$. In this case, by mean the assumption of $\chi(t) = A\,cos\omega t + B\,cos(2\omega t)$ and with appropiate values of A and B it is possible to reproduce the statistical angle, which tune all dependence with the anyonic behavior [3].

Chapter 3

Anyons with local two-body interactions

Keilmann *et al.* study the anyon-Hubbard model with two body-interactions and focus their work on the statistically induced quantum phase transition between Mott-insulator and superfluid phases [1]. From this theoretical study, other interesting problems appears. A proposal for improving the experimental realization of Keilmann and co-workers [2], the systematic study of the pseudo-anyon-Hubbard model on a one-dimensional lattice [52] and the numerical demonstration of the existence of a nontrivial topological Haldane phase for anyons in the one-dimensional extended Hubbard model with a mean density of one particle per site [53]. We observed that it is necessary to find a tool that gives us a better estimate of the critical point than simply the gap closing. We studied the phase transition using the block von Neumman entropy.

3.1. Phase diagram

The anyon-Hubbard model takes into account the hopping of the anyons along the lattice and the local two-body interaction between them [1], and its Hamiltonian is given by

$$H = -t\sum_{j}^{L-1}\left(a_j^{\dagger}a_{j+1} + h.c\right) + \frac{U}{2}\sum_{j}^{L} n_j(n_j - 1), \tag{3-1}$$

where $t > 0$ is the tunneling amplitude connecting two neighboring sites, U is the on-site interaction, L is the length of the lattice, n_j is the number operator.

The fractional version of a Jordan-Wigner transformation [1]

$$a_j = b_j\ exp\left(i\theta\sum_{i=1}^{j-1} n_i\right), \tag{3-2}$$

where the operator b_j describes spinless bosons, which satisfy $[b_j, b_i^\dagger] = \delta_{ji}$ and $[b_j, b_i] = 0$. The number operator is defined by $n_i = a_i^\dagger a_i = b_i^\dagger b_i$.

After using the anyon-boson mapping (3-2), the anyon-Hubbard Hamitonian is given in terms of bosonic operators thus:

$$H = -t\sum_{j}^{L-1}\left(b_j^\dagger b_{j+1} e^{i\theta n_j} + h.c.\right) + \frac{U}{2}\sum_{j}^{L} n_j(n_j-1). \tag{3-3}$$

To calculate the ground state of a lattice with L sites and N particles, we truncated the local Hilbert space by considering only $\rho+5$ states when the density of the particles is $\rho = N/L$ [55] and used the finite-size density matrix renormalization group algorithm (DMRG) with open boundary conditions. Also, we used the dynamical block state selection (DBSS) protocol based on a fixed truncation error of the subsystem's reduced density matrix instead of using a fixed number of preserved states in the DMRG sweeps [56]. Using this protocol, we obtained a discarded weight of around 10^{-9} or less, and the maximum number of states retained was $m = 1080$. We fix the energy scales by considering $U = 1$.

In the context of the quantum Hall regime, an experimental setup with a superconducting film adjacent to a two-dimensional electron gas can be understood in terms of anyons with a statistical angle $\theta = \pi/4$, and this system could prove useful in schemes for fault-tolerant topological quantum computation [57]. A mean-field calculation of the phase diagram of one-dimensional anyons for densities $\rho = 1, 2$, and 3 was presented by Keilmann *et al.* for $\theta = \pi/4$ [1]. The above facts motivated us to consider this special angle in the first part of our study.

First of all, it is important to observe that, for $\theta = 0$ the anyon-Hubbard (3-3) model corresponds to the well-known Bose-Hubbard model in this limit. Many analytical and numerical approaches have been used to study the ground state of the Bose-Hubbard model, and we know that for large t, the bosons would be completely delocalized in the lattice and the system would be in a superfluid state. When U dominates, an integer number of bosons would be localized at each site, and the ground state is a Mott insulator one. The border between the superfluid and the Mott insulator regions can be estimated with the energy for adding and removing particles:

$$\begin{aligned} \mu^p(L) &= E_0(L, N+1) - E_0(L, N), \\ \mu^h(L) &= E_0(L, N) - E_0(L, N-1), \end{aligned} \tag{3-4}$$

where $E_0(L, N)$ denotes the ground-state energy for L sites and N particles. If the above parameters (L and N) are finite, we observe that the single-particle excitations exhibit a

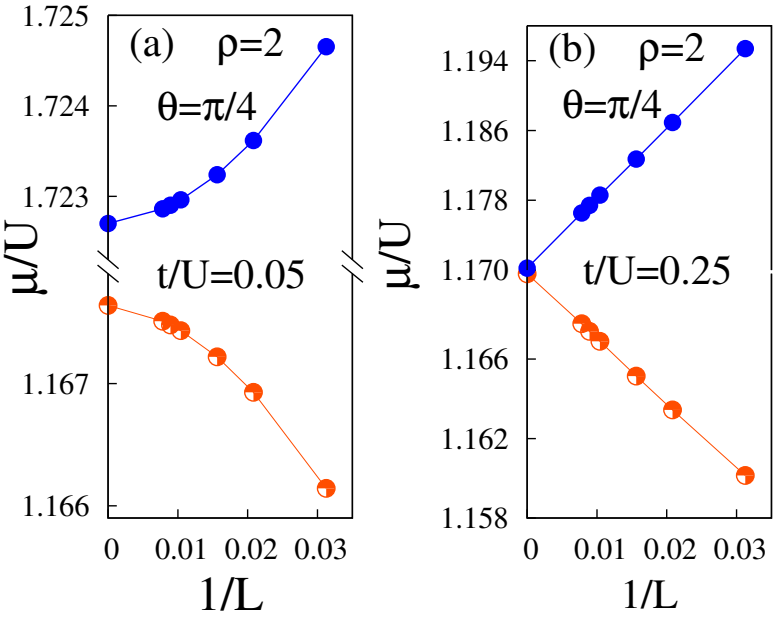

Figure 3-1: System size dependence of the chemical potential of anyons in 1D with statistical angle $\theta = \pi/4$ and $\rho = 2$. The upper set of data in each panel corresponds to the particle excitation energy and the lower one to the hole excitation energy. In the left panel ($t/U = 0.05$), we show a state with a finite difference at the thermodynamic limit, while this difference vanishes in the right panel($t/U = 0.25$).

finite gap $\Delta\mu(L) = \mu^p(L) - \mu^h(L) = E_0(L, N+1) + E_0(L, N-1) - 2E_0(L, N)$. A Mott insulator state is achieved if the density of the system $\rho = N/L$ is an integer and at the thermodynamic limit $\Delta\mu = lim_{L,N\to\infty}\Delta\mu(L) > 0$. By contrast, the superfluid phase is gapless.

The evolution of the energies for adding and removing particles given by Eq. (3-4) versus the inverse of the lattice length for anyons with $\theta = \pi/4$ and density $\rho = 2$ appear in Fig. 3-1. In each panel, the upper (lower) curve corresponds to the energy for adding (removing) particles. Regardless of the value of the hopping parameter, we obtained that the energy for adding (removing) particles always decreases (increases) as a function of $1/L$; however, this evolution is quadratic for $t/U = 0.05$, and at the thermodynamic limit we obtain $\Delta\mu/U = lim_{L,N\to\infty}[\mu^p(L) - \mu^h(L)] = 0.55$, which suggests that the ground state corresponds to a Mott insulator one. On the other hand, for $t/U = 0.25$, the evolution is linear, the energy for adding and removing particles meets at the thermodynamic limit, and the ground state is superfluid. This figure tells us that the anyon liquid passes from a Mott insulator state to a superfluid one when the kinetic energy increases; hence its behavior is similar to the Bose-Hubbard model ($\theta = 0$), and the main difference will be the position of the critical point.

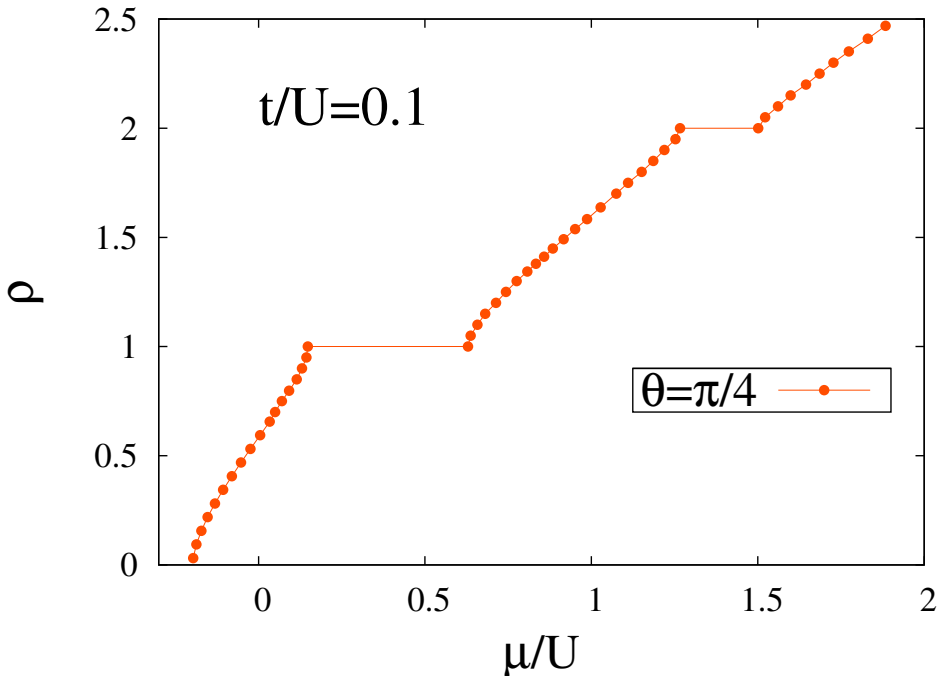

Figure 3-2: Density ρ versus chemical potential μ at the thermodynamic limit for $t/U = 0.1$ and a statistical angle $\theta = \pi/4$.

In Fig. **3-2**, we show the density ρ as a function of the chemical potential, which was found at the thermodynamic limit. We observe that the chemical potential increases as the density grows; however this behavior changes when the density reaches integer values. For $\rho = 1$ and $\rho = 2$, we obtain two plateaus in the curve, which indicates that the ground state has a finite gap for integer densities, whereas the width of these plateaus give us the value of the gap. Comparing this with Fig. **3-1**, we obtain that for a ground state with two bosons per site, the gap will decrease monotonously as the hopping parameter increases. An important fact in Fig. **3-2** is that the slope is always greater than zero, i. e. the compressibility $\kappa = \partial\rho/\partial\mu > 0$, an argument that is related to the absence of first-order transition. Note that Batrouni and his collaborators have shown the existence of first-order phase transitions ($\kappa < 0$) in two-dimensional system of spinless [58] and spinor [59] bosons, but for even lobes in one-dimensional systems of spin-1 bosons, the compressibility is positive and the phase transition is of first order, this being caused by the spin degree of freedom [60]. Taking into account the above discussion and our numerical results, we believe that the phase transitions for $\theta = \pi/4$ are of the second order kind; however the possibility of find first-order transitions in the anyon-Hubbard model for larger values of θ and/or a fixed number of particles is an interesting open problem.

The mean-field phase diagram of Hamiltonian found by Keilmann *et al.* [1] is reproduced in Fig. **3-3** (gray squares). For $\theta = \pi/4$, we note that the Mott insulator lobes are surrounded

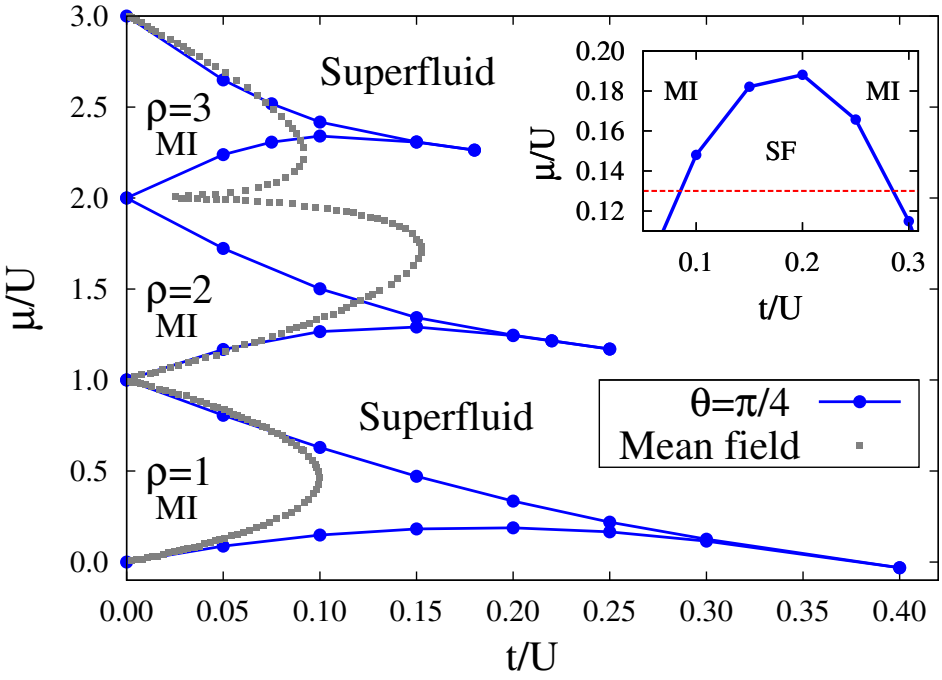

Figure 3-3: Phase diagram of the anyon-Hubbard model with statistical angle $\theta = \pi/4$ for the densities $\rho = 1, 2$, and 3 using DMRG (blue line-circle) and comparison with the mean-field solution (gray squares) for the same densities (mean-field data were taken from [1]). Inset: display sequence from Mott insulator to supefluid and back to Mott insulator for $\theta = \pi/4$ and $\rho = 1$ at fixed $\mu = 0.13$.

by the superfluid phase, and their shapes are rounded. The mean-field solution shows that the critical points for all densities are lower than the ones found for the Bose-Hubbard model, and that the second lobe is larger than the other lobes. This result suggests a possible odd-even asymmetry present in the system in which lobes with an even density ($\rho = 2$) increase in comparison with those with odd densities ($\rho = 1$ and 3). In addition, we can see that the critical point for the densities $\rho = 1$ and $\rho = 3$ do not differ considerably.

Despite the interesting results of the mean-field solution of Hamiltonian (3-3), a determination of the phase diagram for higher densities ($\rho > 1$) beyond mean-field has not been done. For this reason, we calculated the chemical potential at the thermodynamic limit and found the phase diagram for $\theta = \pi/4$ and the three densities $\rho = 1, 2$, and 3 (blue line-circle) at the plane $(\mu/U, t/U)$. For small values of t/U, we see that the borders of the first Mott lobe obtained by mean-field and DMRG are closer; however for larger values the mean-field solution lobe closes, while the DMRG solution stretches slowly, and the gap closes at around $t/U = 0.40$, which is four times larger than the mean-field result [see Fig. **3-3**]. Note that our results are in agreement with the DMRG results of Keilmann *et al.* for $\rho = 1$. For the second lobe, we observe that the mean-field and DMRG solutions only coincide at the lower edge

for small values of t/U. The area of the mean-field solution is greater and the DMRG gap closes at around $t/U = 0.25$, which indicates that there is no odd-even asymmetry between the lobes, this being an artifice of the mean-field solution. For the lobe with density $\rho = 3$, we obtain that the upper borders of both solutions are closer for small values of t/U and the critical point for this density is located around $t/U = 0.18$, which is lower than the location of the critical points for the other densities.

In Fig. **3-3**, we observe that the area of the Mott insulator lobes decreases as the global density of the system increases, which implies that the location of the critical points moves to lower values with the density. These facts are consistent with those obtained for the Bose-Hubbard model [61]. However, the effect of anyonic statistics reflected in a correlated density dependent hopping is larger values of the critical points for all the densities considered, i. e., for a nonzero statistical angle, we need more kinetic energy to delocalize the particles and generate a superfluid state. Note that for all lobes, the gap closes as the hopping parameter increases and the shape of lobes becomes elongated, with a large tip, which indicates that the gap closes very slowly, a fact relevant to determination of the type of phase transition.

In the inset of Fig. **3-3**, we show a zoom of the lower edge of the first lobe and a chemical potential constant line ($\mu/U = 0.13$). Based on this inset, it is clear that the hole excitation energy has a maximum value, a fact repeated for the others lobes, but the position of the maximum moves to lower values of the hopping. Moving on along the red line, we observe that for small values of t/U there is one boson per site, and the ground state is a Mott insulator one, but for bigger values a quantum phase transition takes place and the system passes to a superfluid phase with a global density lower than one. When $t/U \approx 0.28$, the system re-enters into a Mott insulator phase with density $\rho = 1$, and a new transition to a superfluid phase with global density greater than one is expected for larger values of the hopping. Note that this reentrance phase transition also happens for the other lobes calculated here. This fact was first discussed by Kuhner *et al.* for the Bose-Hubbard model ($\theta = 0$) with density $\rho = 1$ [62], and recently a detailed study was conducted by Pino *et al.* [63].

We show the phase diagram for different angles in Fig. **3-4**. The values of the particle and hole excitation energies were extrapolated at the thermodynamic limit. We observe a Mott insulator phase surrounded by a superfluid phase and we reproduce the well-known phase diagram of the Bose-Hubbard model ($\theta = 0$) [61,64]. The Mott lobe grows in both directions with an increase of the angle (leading to anyonization of the gas), implying that the critical point position is shifted to the right. Thus the state-dependent hopping helps to localize the particles. This presents the possibility of inducing a quantum phase transition from the superfluid into the Mott insulator phase by changing the statistical angle and not just by the competition between t and U .

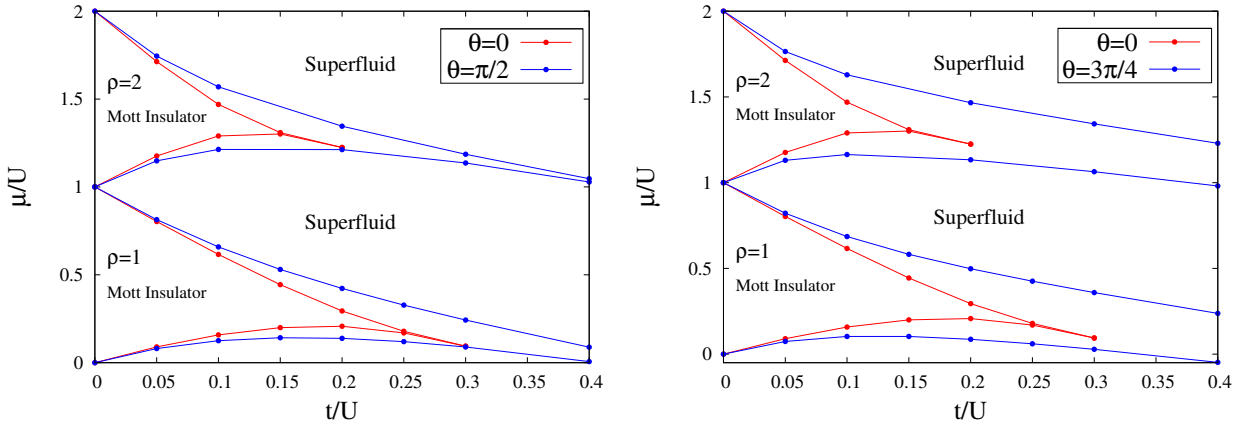

Figure 3-4: Phase diagram of anyons with statistical angle $\theta = \pi/2$ (Left) and $\theta = 3\pi/4$ (right) for the densities $\rho = 1$ and $\rho = 2$. The lines are visual guides and the points are DMRG results.

From the above discussion and the previous papers about the anyon-Hubbard model, we know that the ground state exhibits a Mott insulator phase and a superfluid phase whose boundaries were found here for three different densities considering an angle of $\theta = \pi/4$ (see Fig. **3-3**). However, to use the closing gap criterion to determine the critical point when the density is fixed is not appropriate, as has been widely discussed for the Bose-Hubbard model. The precise determination of the critical points of this last-named model has received significant attention in the last decade, and many approaches have been considered, for instance using the interaction parameter of the Luttinger liquid [61, 62], or the tools of quantum information theory [17, 65, 66]. Clearly, for the scientific community a precise determination of the critical points that separate the two quantum phases for the anyon-Hubbard model is a very interesting problem.

3.2. Entanglement and critical points

Today, entanglement is an important tool for studying the ground state of strongly correlated systems as well as the quantum phase transitions that will occur in the system. Measures of the entanglement, such as fidelity, von Neumann entropy, purity, and negativity, among others have been useful in determining the critical points of diverse models [16]. In the present thesis, we will use the von Neumann block entropy for studying the ground state of the Hamiltonian (3-3).

We consider a system with L sites divided into two parts. Part A has l sites ($l = 1, ..., L$), and the rest form part B, with $L - l$ sites. The von Neumann block entropy of block A is defined by $S_A = -Tr\varrho_A ln\varrho_A$, where $\varrho_A = Tr_B\varrho$ is the reduced density matrix of block

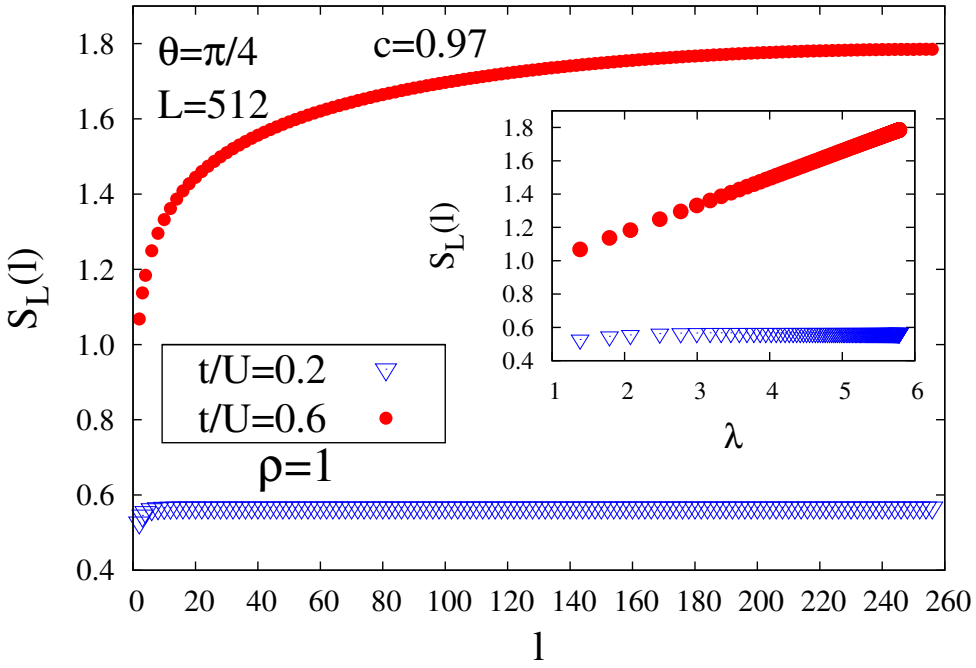

Figure 3-5: The von Neumann block entropy $S_L(l)$ as a function of l for a system with size $L = 512$, $\rho = 1$, and $\theta = \pi/4$. Here we consider two different values of the hopping parameter, $t/U = 0.2$ and $t/U = 0.6$. In the inset, the von Neumann block entropy $S_L(l)$ as function of the logarithmic conformal distance λ is shown, revealing a linear behavior for the critical state. Otherwise, the non-critical state does not exhibit linear behavior, because of the short correlation length. We found that the central charge is $c = 0.97$.

A and $\varrho = |\Psi\rangle\langle\Psi|$ the pure-state density matrix of the whole system. For a system with open boundary conditions, the behavior of the von Neumann block entropy as a function of l depends on the nature of ground state and provides information about the type of phase, because it saturates(diverges) if the system is gapped (gapless) [67], thus:

$$S_L(l) = \begin{cases} \frac{c}{6} ln[\frac{2L}{\pi} sin(\frac{\pi l}{L})] + \Theta, & \text{critical,} \\ \\ \frac{c}{6} ln[\xi_L] + \Theta', & \text{non critical,} \end{cases} \tag{3-5}$$

where c is the central charge and ξ_L is the correlation length. The constants Θ and Θ' are nonuniversal and model dependent.

The von Neumann block entropy $S_L(l)$ as a function of the block size l is shown in Fig. **3-5** for a lattice with global density $\rho = 1$, statistical angle $\theta = \pi/4$, and two different values of the hopping: $t/U = 0.2$ and $t/U = 0.6$. At the limit $t \to 0$, the ground state can be seen as a product of local states, i. e., it is separable, and we expected that the entanglement would be zero. For a nonzero value of the hopping $t/U = 0.2$, we observe that the block entropy

is different from zero; it increases rapidly, and saturates at a certain value, in accordance with the expression Eq. (3-5), which indicates that the ground state has a finite correlation length, as is characteristic of the Mott insulator phase. A different behavior of $S_L(l)$ as a function of l is observed for $t/U = 0.6$; now the von Neumann block entropy always grows with the block size and diverges, which characterizes a critical state.

In the inset of Fig. **3-5**, we show the relationship between block entropy and the logarithmic conformal distance ($\lambda = ln\left[\frac{2L}{\pi} sin\left(\frac{\pi l}{L}\right)\right]$). We obtain a nonlinear dependence for small values of the hopping ($t/U = 0.2$) due to the short correlation length, and linear behavior is observed for the critical state ($t/U = 0.6$). Observing the expression (3-5), we note that the slope of the block entropy versus the logarithmic conformal distance is related to the central charge of conformal theory; hence from the inset of Fig. **3-5** we obtain the central charge $c = 0.97$. This value is very close to 1, which corresponds to the central charge for the Bose-Hubbard model ($\theta = 0$). Specifically, in the supefluid phase the low-energy physics of the one-dimensional Bose-Hubbard model can be described as a Luttinger liquid, which is a conformal field theory with central charge $c = 1$ [17].

When the hopping increases from zero, the von Neumann block entropy allows us to identify two different ground states, one critical and the other not; however, identifying for which value of t/U the transition takes place is not an easy task. Nevertheless, we can calculate the block entropy for different values of t/U and try to estimate the critical value for which the system passes from a saturation behavior to a critical one, which could be a criterion for determining the critical point. In reality, this is very poor and needs a very large number of calculations. This problem was addressed by Läuchli and Kollath, who proposed an estimator in terms of the von Neumann block entropy defined by the following expression: $\Delta S(L) = S_L(L/2) - S_{L/2}(L/4)$. This measures the increase of the entropy at the mid-system interface upon doubling the system size [17]. According to (3-5), we obtain:

$$\Delta S_L(l) = \begin{cases} \frac{c}{6} ln[2], & t \geq t_c, \\ 0, & t < t_c. \end{cases} \tag{3-6}$$

We expect that the behavior of ΔS will be a step function as a function of t/U. Even though other estimators have been proposed in the literature for determining the critical point using the block entropy [68], we follow the Läuchli and Kollath proposal, because it works well for the Bose-Hubbard model.

In Fig. **3-6**, we show the dependency between the estimator ΔS_{LK} and t/U for $L = 256$ and $\rho = 1$ for two angles, $\theta = 0$ and $\theta = \pi/4$. The estimator is zero at $t = 0$ for any value of the statistical angle and remains constant in a finite region. The width of this region depends on the statistical angle, i. e. the width of the Mott insulator area will increase with the angle θ. The estimator grows quickly after a certain value of the hopping, which varies with

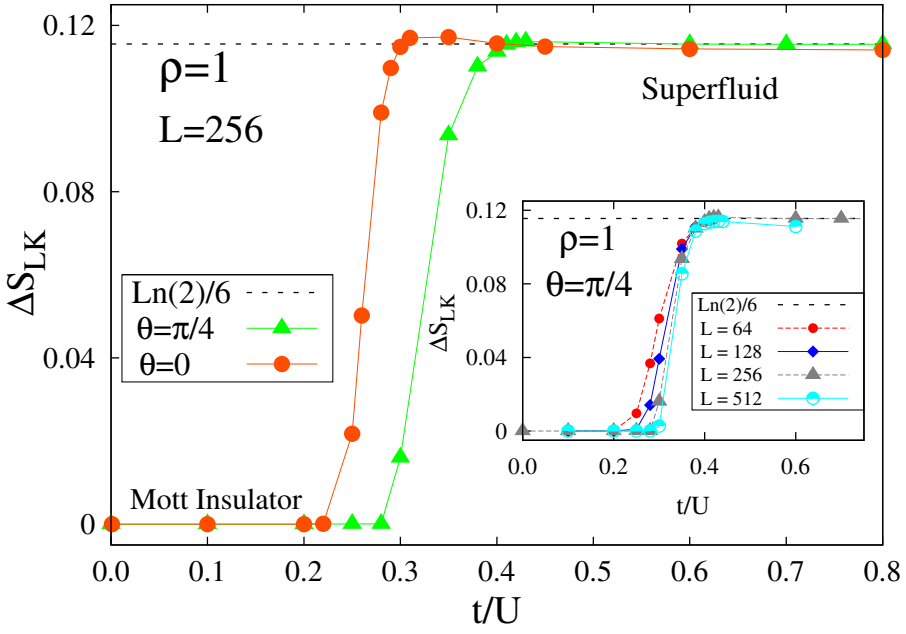

Figure 3-6: The estimator ΔS_{LK} as a function of the hopping parameter t/U for $\theta = 0$ and $\theta = \pi/4$. Here, we fixed L=256 and $\rho = 1$. In the inset, the estimator ΔS_{LK} vs t/U for $\theta = \pi/4$, and different system lengths $L = 64$, 128, 256, and 512. The lines are visual guides.

the statistical angle and reaches the value $ln(2)/6$. This value corresponds to the estimator evaluated in a critical region according to the expression Eq. (3-6). Note that the estimator remains constant at this value for larger values of the hopping. It is clear from the figure that the anyon-Hubbard model exhibits a Mott insulator and a superfluid phase and that the behavior of the estimator corresponds to a step function. The value of the critical point is taken as the first value to reach $ln(2)/6$. In the inset of Fig. **3-6**, we consider different system sizes, from 64 up to 512 sites, and observe that when the system size increases, the hopping for which $\Delta S_{LK} \neq 0$ moves to the right, and the curve tends to a step function as a function of t/U, and so we see that the expected behavior will occur.

We found that the quantum critical point for $\theta = 0$ and $\theta = \pi/4$ are $t_c/U = 0.303$ and $t_c/U = 0.414$, respectively. Note that the result for the bosonic case $\theta = 0$ is in accordance with previous results [61]. It is important to observe that the most accurate determination of the critical point gives us a bigger value in comparison with the calculation shown in Fig. **3-3**, where we observe that the gap closes at $t/U = 0.40$. The estimator results reinforce the idea that the inclusion of state-dependent hopping helps to localize the particles in this system; in other words, the inclusion of the correlated hopping means that the kinetic energy to delocate the system increases, since there is a displacement towards greater t/U of the critical point.

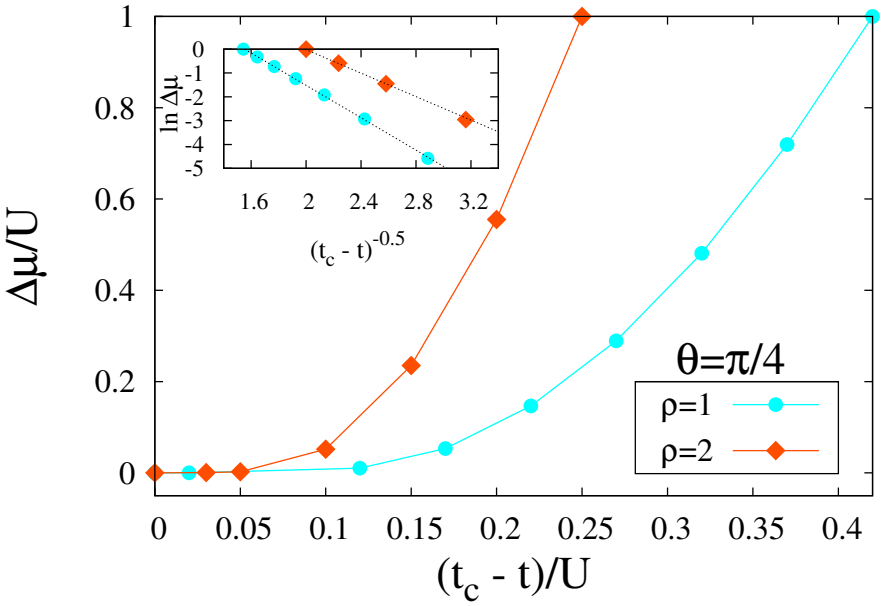

Figure 3-7: Energy gap as a function of $t_c - t$ for $\rho = 1$ and $\theta = \pi/4$. In the inset, $ln\ \Delta\mu$ vs $1/\sqrt{t_c - t}$. Here, the points are DMRG results, and the fits to the Kosterlitz-Thouless transition are shown by lines.

We have characterized the quantum phases of the anyon-Hubbard model with $\theta = \pi/4$, and we have shown that the use of the Läuchli and Kollath estimator allows us to better find the t_c/U position for the case $\rho = 1$. On the other hand, we showed that the central charge c in the critical phase is very close to 1. However, the kind of transition that is taking place has not yet been discussed. It is important to remember that for a fixed integer number of particles, the Bose-Hubbard model belongs to the universality class of the XY model; hence the gap closes following a Kosterlitz-Thouless formula [69]. We present the energy gap $\Delta\mu/U$ as a function of $(t_c - t)/U$ for anyon-Hubbard model with $\theta = \pi/4$ and for densities $\rho = 1$ and $\rho = 2$ in Fig. **3-7**. We found the critical point for $\rho = 2$ following the same procedure used to determine the critical point for $\rho = 1$. Regardless of the density, we obtained that the gap exhibits a linear dependence for larger values of $(t_c - t)/U$; however, as the parameter diminishes, the gap decreases smoothly, and finally we observe that the gap vanishes very slowly, corroborating the results shown in Fig. **3-3**. The above results obtained for the anyon-Hubbard model suggest that we try to fit the curves in Fig. **3-7** to the Kosterlitz-Thouless formula:

$$\frac{\Delta\mu}{U} = \frac{\mu^p - \mu^h}{U} \sim exp\left(\frac{const.}{\sqrt{(t_c - t)/U}}\right). \tag{3-7}$$

In the inset of Fig. **3-7**, we present $ln\ (\Delta\mu/U)$ as a function of $1/\sqrt{(t_c - t)/U}$, which shows

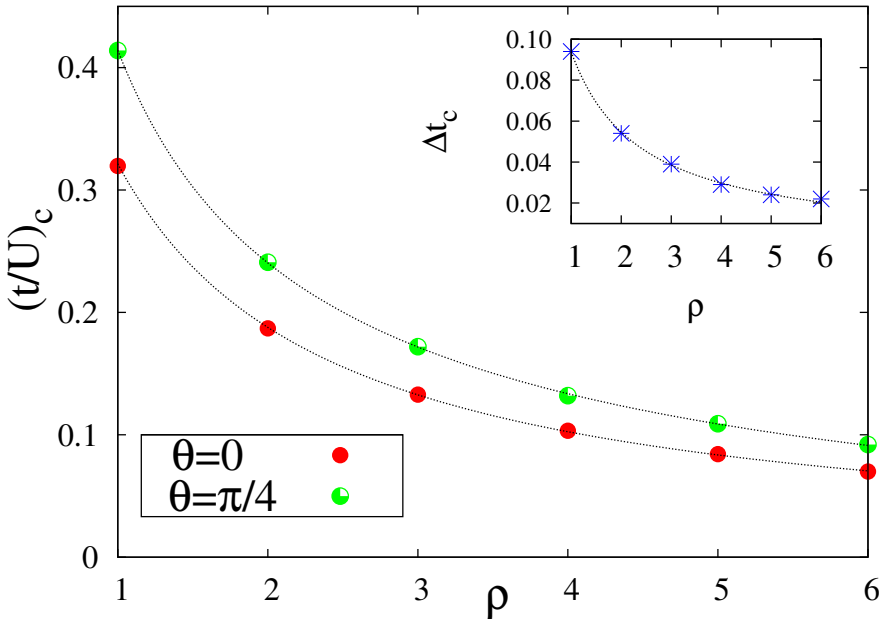

Figure 3-8: Quantum critical point position $(t/U)_c$ as a function of the density for the anyon-Hubbard model with $\theta = \pi/4$ and $\theta = 0$. The dashed lines represent the best fit of the numerical data with the function of Eq. (3-8). The numerical constants obtained for $\theta = \pi/4$ are $(\alpha, \beta, \gamma) = (-0.037, 0.45, -0.7)$ Inset: Δt_c between $\theta = 0$ and $\theta = \pi/4$ as a function of the density ρ. (the data of $\theta = 0$ were taken from [4])

a linear dependence for both densities. Therefore, we affirmed that the transitions are of the Kosterlitz-Thouless kind for these densities under the parameters considered. The above result and the fact that the central charge is close to 1 allow us to infer that the anyon-Hubbard model with $\theta = \pi/4$ is in the same universality class as the Bose-Hubbard model.

In Fig. **3-3**, we show that the position of the critical points moves to lower values as the density increases. It is noteworthy that the functional dependency of the critical points of the superfluid-to-Mott-insulator transition with the density for the Bose-Hubbard was a problem addressed by Danshita *et al.* in 1D, 2D, and 3D [4]. They found that the critical values versus the density are well approximated by the function $\left(\frac{U}{D\rho t}\right)_c = a + b\rho^{-c}$, where D denotes the dimensionality of the system and the constants a, b, and c are numerically determined. We wanted to find out whether the expression obtained by Danshita *et al.* is valid for the anyon-Hubbard model with $\theta = \pi/4$, so we increased the local Hilbert space, considering $\rho+5$ states when the ground state with ρ particles per site is taken into account. This correction allows us to determine the critical points with more precision; however, the computational cost increases. Using the estimator (3-6) to find the critical points for higher densities, we obtain the results shown in Fig. **3-8** for a fixed value of the statistical angle

($\theta = \pi/4$) and its comparison with the bosonic case $\theta = 0$ (data taken from [4]). We can see how as the density increases, the position of the critical point moves toward progressively smaller t values, which implies that the insulator region decreases as we increase the filling factor of the system. Within the interval of densities studied, the curve for anyons is above the curve for bosons. This implies that the Mott lobe is always greater for the anyon case. Nevertheless, as we increase the density, the difference between the critical points decreases.

The best fit of the numerical data of Fig. 3-8 was obtained using the relation

$$\left(\frac{t}{U}\right)_c = \alpha + \beta\rho^{-\gamma}, \tag{3-8}$$

with $\alpha = -0.037$, $\beta = 0.45$, and $\gamma = -0.7$ for the anyon case ($\theta = \pi/4$). Note that the above expression is different from the general formula found by Danshita *et al.*. We see in the inset of Fig. 3-8 the difference between the critical point positions of the Bose- and anyon-Hubbard model. This quantity decreases as the density grows and does not cancel out, which reflects the influence of the density-dependent hopping.

Due to the above mentioned motivation, we concentrated our study of the anyon-Hubbard model on the statistical angle $\theta = \pi/4$, but now we want to explore the evolution of the critical point position as a function of the angle, and so we consider larger values of the statistical angle, as is shown in Fig. 3-9. There, we present the results of the Läuchli and

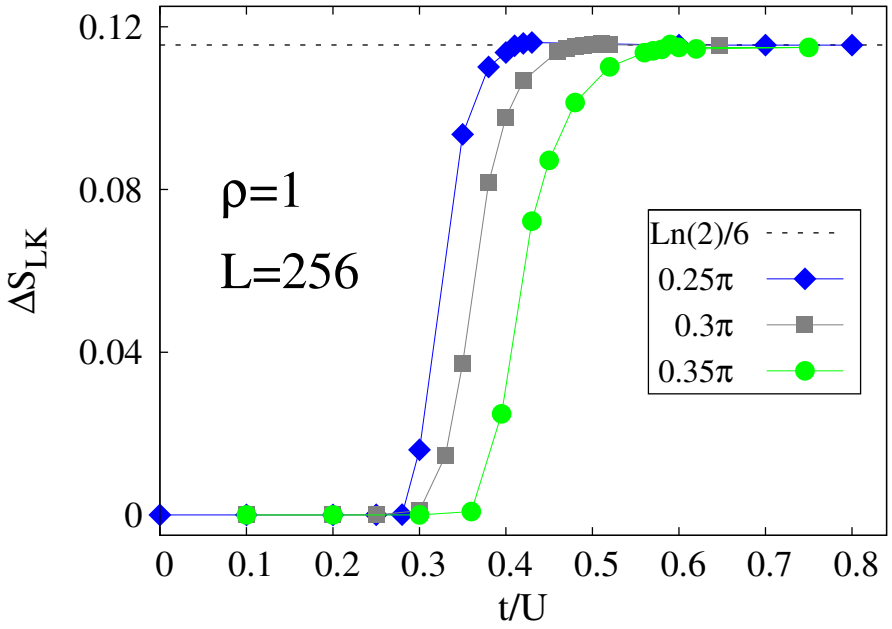

Figure 3-9: The estimator ΔS_{LK} as a function of the hopping parameter t/U for various statistical angles $\theta = 0.25\pi, 0.3\pi$ and 0.35π. Here, we fixed L=256 and $\rho = 1$.

Kollath's estimator ΔS_{LK} as a function of t/U for a system with one boson per site and three different values of the statistical angle were considered. Regardless of the θ value, the behavior of the estimator is similar. We observe that it is zero in a finite region of t/U values, indicating that the system is in a Mott insulator state in this region. Note that the size of this region increases with the angle in a nonlinear proportion. After a certain value, which depends on the statistical angle, the estimator increases quickly and reaches the value of $(ln\ 2)/6$. For larger values of t/U, the estimator remains constant at the latter value, which indicates that the system is in a superfluid state, in accordance with the expression Eq. (3-6). Although the results shown in this figure correspond to a lattice size of $L = 256$, we expected that for bigger lattices this behavior would be maintained, and a step function would be obtained in a manner similar to the inset of Fig. **3-6**. On the other hand, we observe that the number of the states per block to reach the limit value $(ln\ 2)/6$ increases dramatically with the statistical angle. From Fig. **3-9**, we confirm that particles tend to localize when the statistical angle grows, a fact that is marked by an increase in the Mott insulator lobes area; therefore, the position of the critical point moves to larger values.

Using the vanishing gap criteria, Keilmann *et al.* estimate the evolution of the critical points as a function of the statistical angle for a global density $\rho = 1$, showing that critical strength U_c/t decreases with θ and vanishes at $\theta = \pi$ [1]. Today, we know that the above first approximation criterion is not very accurate, and taking into account that the Läuchli and Kollath estimator allows identify the border between the Mott insulator and the superfluid phases, we study the evolution of the critical points as the statistical angle increases in a chain with one or two particles per site (Fig. **3-10**). We observe that the critical point increases gradually and smoothly with θ, regardless of the global density ρ, which reflects the increase in the localization of the particles. The effect of the repulsion between the particles is evident in Fig. **3-10**, since for $\rho = 2$ more particles interact and the required kinetic energy to pass to the superfluid state is less than for the $\rho = 1$ case for any value of θ. Note that the position of the critical points for $\rho = 2$ moves to greater values more slowly than in the $\rho = 1$ case as the statistical angle increases. When we compare the position of the critical points for the first Mott lobe found by Keilmann *et al.* with our results, we observe that for small (large) angles our critical point position moves to lower (greater) values compared to the Keilmann *et al.* results.

We study the anyon-Hubbard model using the density matrix renormalization group (DMRG) method. Using the energy for adding and removing particles in the system, we construct the phase diagram for $\theta = \pi/4$ in the plane $(t/U,\ \mu/U)$ for three densities ($\rho = 1, 2$, and 3) and we conclude that as we increase the density, the position of the critical point changes to lower values of kinetic energy t/U. These results contrast with previous mean-field calculations for $\theta = \pi/4$ [1]. On the other hand, the phase transition was studied using the block von Neumman entropy, we use the estimator proposed by Läuchli and Kollath [17] to determine the

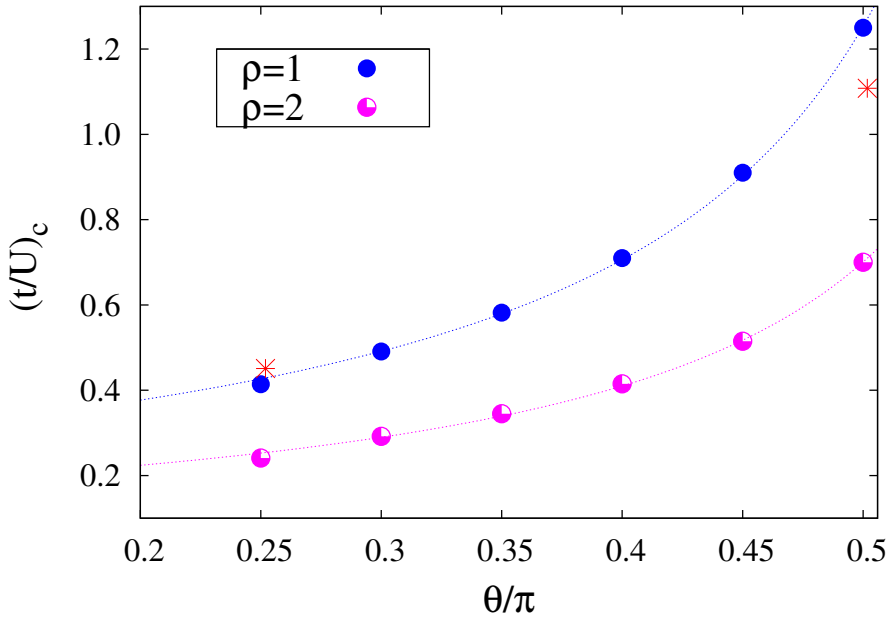

Figure 3-10: Critical point evolution with statistical angle θ for the anyon-Hubbard model. The dashed lines represent the best fit of the numerical data. The stars represent the critical points found by Keilmann *et al.* We can not explore larger values of θ due to the dramatic increase in the number of states that must be maintained in order to achieve the limit $(ln\ 2)/6$.

critical points of the anyon-Hubbard model. We obtain the evolution of the critical points with the density and find functional relationships between the different parameters that the Hamiltonian depends on. We show that a simple analytical function is a good approximation of the results. It is important to note that studies related to the most precise estimation of critical points have not been previously reported, beyond the gap closing. We use the critical points and show that the Kosterlitz-Thouless formula is suitable for describing the closing of the gap, and we can infer that the anyon-Hubbard model with $\theta = \pi/4$ is in the same universality class as the Bose-Hubbard model.

Chapter 4

Anyons with local three body interactions

It is important to highlight that experimental with ultracold atomic gases in optical lattices have advanced to the point that many-body models can be engineered microscopically. As a result to consider these many-body terms in Hamiltonians, appears exotic quantum phases and open a new route for theoretical and experimental frameworks [21–23]. In this way, Buchler *et al.* showed that polar molecules in optical lattices can be tuned to a regime where the three-body interactions are dominant [23], this many-body system provides an example where three-body interactions play the dominant role and the the two-particle interaction can be independently controlled [23]. Moreover, Johnson *et al.* showed that there are effective three- and higher-body interactions generated by the two-body collisions of atoms [24]. On the other hand, evidence was found of multi-body interactions using an interferometric technique for ^{87}Rb atoms confined in an optical lattice [25]; the measurements of multi-body interaction energies provides crucial input for the comparison of optical-lattice quantum simulators with many-body quantum theory [25]. Recently, was present a simple, experimentally realizable method to make coherent three-body interactions dominate the physics of an ultracold lattice gas. This scheme allows to reduce or turn off two-body interactions in a rotating frame, promoting three-body interactions [20].

An unexplored problem consists of considering delocalized anyons in a one-dimensional optical lattice under local three-body interactions. This problem it is interesting because the three-body interactions between spinless or spinor bosons cannot generate a Mott insulator state with one particle per site and also change the phase diagram. On the other hand, it has been shown that the anyonic statistics localize the particles, and this can induce a quantum phase transition in systems with two-body interactions. In the present chapter, we study the interplay between the above phenomena and write a Hamiltonian with two terms: the local three-body interaction and the kinetic energy using DMRG.

4.1. Entanglement and phase diagram

The fractional version of the Jordan-Wigner transformation is an exact mapping between anyons and bosons in one-dimension [1]:

$$a_j = b_j \; exp\left(i\theta \sum_{i=1}^{j-1} n_i \right). \tag{4-1}$$

where the operator b_j describes spinless bosons, which satisfy $[b_j, b_i^\dagger] = \delta_{ji}$ and $[b_j, b_i] = 0$. The number operator is defined by $n_i = a_i^\dagger a_i = b_i^\dagger b_i$.

We used this exact mapping and we studied the anyon-Hubbard Hamitonian in terms of bosonic operators. One aspect that should be highlighted is that, due to the fact that the particles in the same site behave like ordinary bosons, and that the local operators do not become modified when the Jordan-Wigner fractional version is used, it is possible to conceive of a modification of the local interaction because only the number operator is being involved. In our case, we introduced an anyon-Hubbard model with local three-body interaction:

$$H \;=\; -t \sum_j^{L-1} \left(a_j^\dagger a_{j+1} + h.c. \right) + \; \frac{W}{6} \sum_j^{L} n_j(n_j-1)(n_j-2), \tag{4-2}$$

This Hamiltonian study the hopping dynamics of anyons in one-dimensional optical lattice considering a repulsive local three-body interactions. The first term in the Hamiltonian (4-2) is the kinetic energy with strength t (hopping amplitude), the second term stems from the short-range interaction between three particles. $W = 1$ is our energy scale.

Using the anyon-boson mapping (4-1) the anyon-Hubbard Hamitonian with three-body interaction is given in terms of bosonic operators thus:

$$H \;=\; -t \sum_j^{L-1} \left(b_j^\dagger b_{j+1} e^{i\theta n_j} + h.c. \right) + \; \frac{W}{6} \sum_j^{L} n_j(n_j-1)(n_j-2). \tag{4-3}$$

We study the ground state of Hamiltonian (4-3) a lattice with L sites and N particles, we truncated the local Hilbert space by considering only $\rho + 5$ states when the density of the particles is $\rho = N/L$ [55]. We used the finite-size density matrix renormalization group algorithm (DMRG) with open boundary conditions. Also, we used the dynamical block state selection (DBSS) protocol based on a fixed truncation error of the subsystem reduced density matrix instead of using a fixed number of preserved states in the DMRG sweeps [56]. Using this protocol, we obtained a discarded weight of around 10^{-10} or less, and the maximum number of states retained was $m = 1200$.

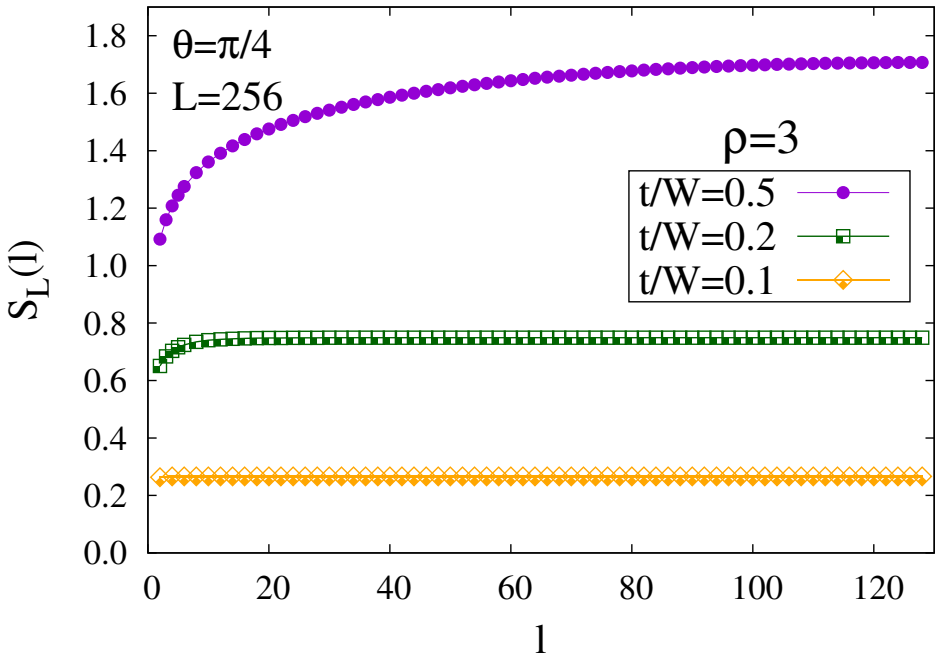

Figure 4-1: The von Neumann block entropy $S_L(l)$ as a function of l for an anyon chain with $\theta = \pi/4$, $\rho = 3$ and size $L = 256$. Here we consider three different values of the hopping parameter, $t/W = 0.1, 0.2$, and 0.5. Clearly, we can see that a change of state happens as the hopping grows.

The evolution of the von Neumann block entropy $S_L(l)$ as the size of the block increases is shown in Fig. 4-1 for a lattice with global density $\rho = 3$, statistical angle $\theta = \pi/4$, and three different values of the hopping: $t/W = 0.1$, $t/W = 0.2$, and $t/W = 0.5$. For small values of the hopping parameter, we expected that the particles would tend to localize and the entanglement would be small. This happened for $t/W = 0.1$, and we observed that the von Neumann block entropy saturates very quickly and has a small value. The above behavior continues for larger values of the hopping parameter ($t/W = 0.2$), but the maximum numerical value is larger, indicating that the entanglement has increased. These results indicate that for a wide range of values of the hopping the system remains in a phase characterized by a finite correlation length, in accordance with the expression Eq. (3-5). However, things change for larger values. For $t/W = 0.5$, the von Neumann block entropy increases smoothly and tends to diverge with the block size, which characterizes a critical state. In this way, the calculation of the von Neumann block entropy allows us to distinguish between two quantum phases in the system (one critical and the other non-critical) and thus to discern the appearance of a phase transition as we increase the tunneling of the particles. This is deduced from the fact that the entropy changes its behavior (saturate-diverge) when we increase the value of t/W. In this case, considering that the system density is an integer and that we are facing a non-critical phase, the results suggest that the system could be found to be in a

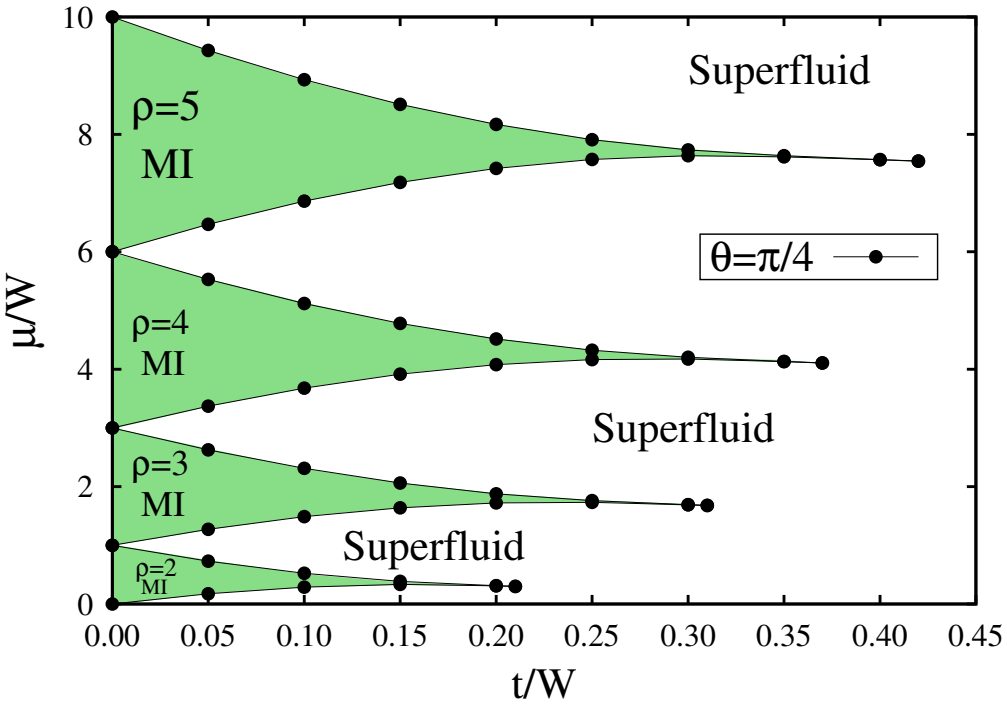

Figure 4-2: Phase diagram of the anyon-Hubbard model with local three-body interactions for $\theta = \pi/4$ and for the densities $\rho = 2, 3, 4$ and 5. The points correspond to extrapolations to the thermodynamic limit from DMRG data and the lines are visual guides. MI means Mott insulator regions.

Mott-insulator phase characterized by having a finite-correlation length. This would explain the fact that the block entropy increases and saturates rapidly at a constant value. On the contrary, in the critical region, the system could exhibit a superfluid state, characterized by a divergent behavior of the von Neumann block entropy and the delocalization of the particles along the lattice. In conclusion, for a fixed global density ρ, the anyon-Hubbard model with local three-body interactions exhibits a Mott insulator to superfluid transition for a finite value of t/W.

The phase diagram of anyons in one dimension under two-body interactions shows Mott lobes surrounded by superfluid regions, with the Mott areas decreasing as the global density grows. In particular, it was found that the critical point for a statistical angle $\theta = \pi/4$ and a fixed global density $\rho = 3$ is located at $t/U = 0.172$, $U = 1$ being the strength of the two-body interactions and the energy scale for this case [1, 26]. In Fig. **4-1**, we observe that the Mott lobe for $\rho = 3$ survives for values greater than $t/W = 0.2$, which indicates that the Mott lobes with three-body interactions will be larger than the lobes with two-body interactions, indicating that three-body interactions generate a larger localization in the system, in accordance with previous results for bosons with three-body interactions.

We found that the Hamiltonian problem (4-3) exhibits Mott and superfluid states, which are characterized by the presence or the lack of an excitation gap at the thermodynamic limit. For a lattice with finite size, the excitation gap is $\Delta\mu(L) = \mu^p(L) - \mu^h(L) = E_0(L, N+1) + E_0(L, N-1) - 2E_0(L, N)$, where $E_0(L, N)$ denotes the ground-state energy for L sites and N particles. In particular, a Mott-insulator phase is characterized by the presence of a positive gap at the thermodynamic limit, since the global density is an integer, while the superfluid phase is characterized by the fact that no gap exists at the thermodynamic limit.

In Fig. **4-2**, we show the thermodynamic limit values of the chemical potential of adding (μ^p) and removing (μ^h) a particle as a function of the hopping for a statistical angle $\theta = \pi/4$ and different global densities ρ. As is well known, the gapped regions are surrounded by superfluid (gapless) ones, and we obtained that upon increasing the global density, the insulator lobes increase and the position of the critical points moves to greater values of t/W in a manner similar to the boson problem ($\theta = 0$) [70], but for anyons the critical points are greater than for bosons. These results indicate that the three-body interaction and the statistics favor the localization of particles and that greater kinetic energy is required to delocalize the particles and generate superfluid states. Another characteristic of Fig. **4-2** is the absence of the insulator region for $\rho = 1$, which is due to the fact that the quantum fluctuations, having on average only one particle per site ($\rho = 1$) and $\theta = \pi/4$, are insufficient for generating particle localization. The elongated shape of the Mott-insulator lobes indicates that the gap closes slowly and possibly follows a Kosterlitz-Thouless formula [26]. The length of the Mott regions on the vertical axis at $t/W = 0$ varies with the density of the system. It is notable that for the Bose- and anyon-Hubbard models with two-body interaction, this length does not change with the density. Rather, it is constant and equal to one in the scale of μ/U. When we consider three-body interactions, the length of the lobe with global density ρ at $t/W = 0$ is $\rho - 1$ for both bosons and anyons with $\theta = \pi/4$.

One of the main findings in the anyon-Hubbard model is that the statistics favor the localization of the particles, which is reflected in the increase in the area of the Mott lobes as the statistical angle θ tends toward π [1]. The absence of the $\rho = 1$ Mott insulator lobe in spinless or spinor bosons chains under local three-body interactions is a very well-known result, but in the present thesis, our subject of study consist of anyons, and we expected that the statistical angle would generate new findings. Hence we wanted to explore if for $\theta > \pi/4$ new insulator phases can appear. Taking into account the above, we fix the statistical angle to $\theta = 3\pi/4$ and study the evolution of the chemical potential as the number of anyons increases. This leads us to Fig. **4-3**, where we show the global density as a function of the chemical potential at the thermodynamic limit. Note that as we increase the overall density of the system, the chemical potential increases for all the non-integer densities, but for a global density $\rho = 1$ a plateau appears, which indicates the existence of a finite gap at the thermodynamic limit for

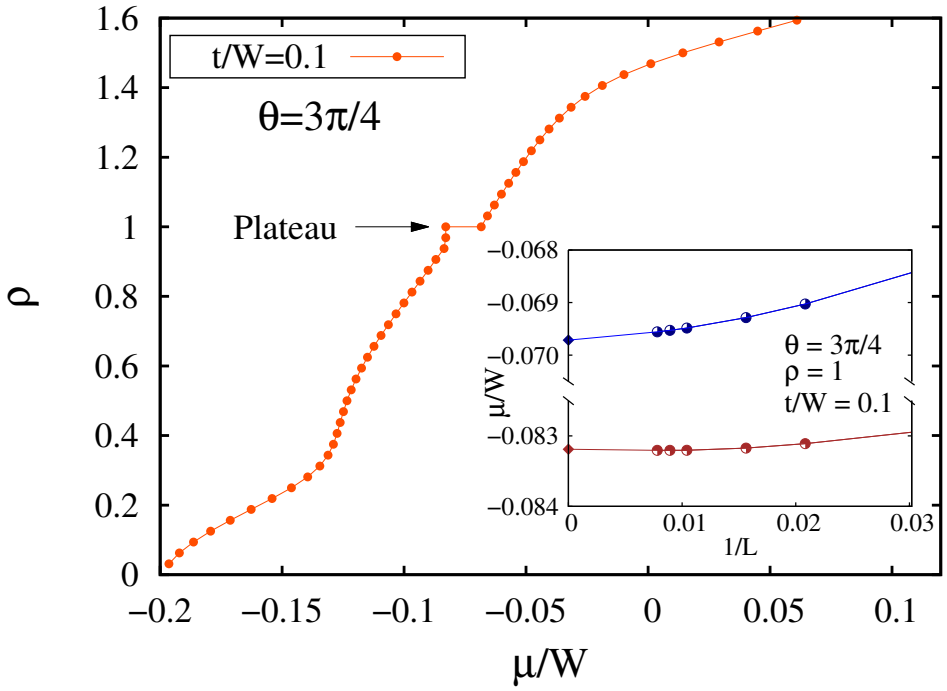

Figure 4-3: Global density ρ versus the chemical potential μ/W for $t/W = 0.1$ and a statistical angle $\theta = 3\pi/4$. The system exhibits a Mott plateau at integer density $\rho = 1$. Inset: System size dependence on the chemical potential of anyons with three-body interactions for statistical angle $\theta = 3\pi/4$ and $\rho = 1$. The upper set data correspond to the particle excitation energy and the lower to the hole excitation energy (the lines are visual guides). The values for $1/L = 0$ (diamonds) correspond to an extrapolation to the thermodynamic limit.

this density given by the width of the plateau. In the inset of Fig. 4-3, we show the evolution of the energies for adding (μ^p) and removing (μ^h) particles versus the inverse of the lattice size for anyons with $\theta = 3\pi/4$ and density $\rho = 1$. This evolution is quadratic for $t/W = 0.1$, and at the thermodynamic limit we obtain $\Delta\mu/W = lim_{L,N\to\infty}[\mu^p(L) - \mu^h(L)] = 0.0135$, which corresponds to the width of the plateau and allows us to conclude that the ground state for $\theta = 3\pi/4$ and $\rho = 1$ is an insulator.

Fixing the hopping parameter to $t/W = 0.1$, we can compare Figs. 4-2 and 4-3 and observe that the quantum fluctuations are very small for $\theta = \pi/4$. Therefore, the interaction term is unimportant and the ground state is a superfluid (gapless), and the first insulator state is obtained for a global density of $\rho = 2$. However, as the statistical angle increases, the particles are more localized, the effect of the interaction term grows, and an insulator state is obtained for $\rho = 1$. The above insulator state is surrounded by gapless regions (see Fig. 4-3), but we note that the evolution is different for values greater than or less than $\rho = 1$, and also for $\rho < 1$ two diverse regions can be identified, which indicates that the increase of

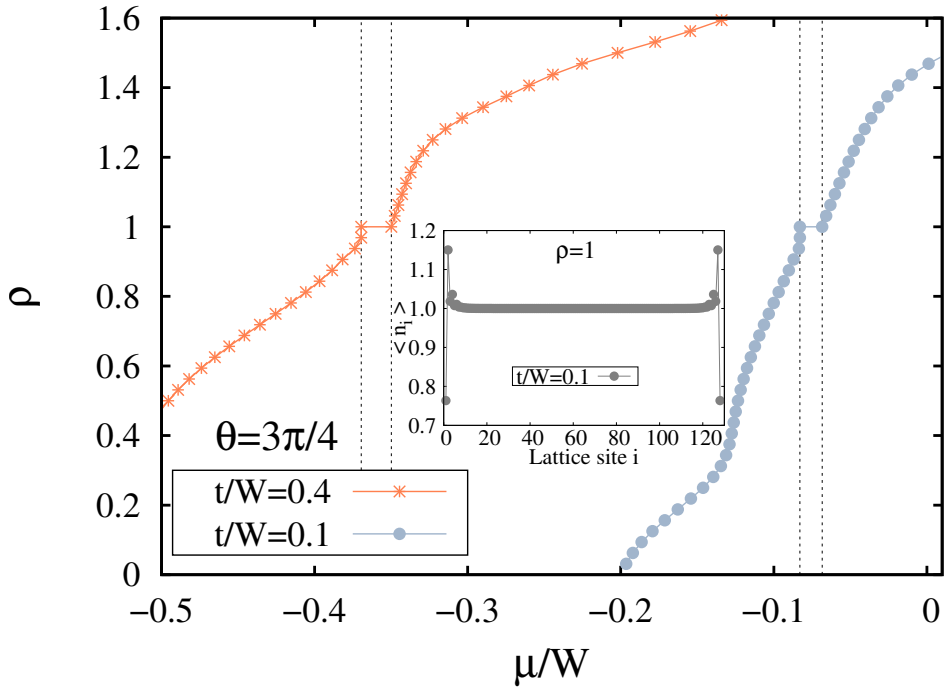

Figure 4-4: Global density ρ as a function of the chemical potential μ/W at the thermodynamic limit. Here, we fix the statistical angle to $\theta = 3\pi/4$ and consider $t/W = 0.1$ and $t/W = 0.4$. The vertical dashed lines delimit the insulator phases. In the inset, we show the density profile along the lattice for $\theta = 3\pi/4$, $t/W = 0.1$ and $L = 120$.

the statistical angle enriches the superfluid regions.

Up to this point, we have found that the statistics generate an insulator state at a global density $\rho = 1$ from a finite value of θ, but we haven't determined other characteristics of this insulator state. To do this, we calculate the density profile of the particles along a lattice of $L = 120$ with $\theta = 3\pi/4$ and $t/W = 0.1$ (see inset Fig. 4-4). At the ends of the lattice, we note strong fluctuations due to the open boundary conditions considered in our study. Despite this, we obtain that at each site there is one particle, i. e. $< n_i >= 1$. This result, as well as the fact that there is a finite gap at the thermodynamic limit, allows us to conclude that the ground state is a Mott insulator, which is generated by the statistics, because for spinless and spinor bosons under local three-body interactions it is impossible to obtain a Mott insulator lobe with $\rho = 1$. To distinguish the Mott regions from the superfluid ones, we draw vertical lines in Fig. 4-4, which shows the global density as a function of the chemical potential at the thermodynamic limit for $\theta = 3\pi/4$ and two different values of the hopping $t/W = 0.1$ and $t/W = 0.4$. From this figure it is clear that a quantum phase transition from a Mott insulator to a superfluid phase will take place, and we observe that for both values of t/W the compressibility ($\kappa = \partial\rho/\partial\mu$) is always greater than zero, which indicates the absence of a first-order transition. Also, we obtained that the overall behavior of the global

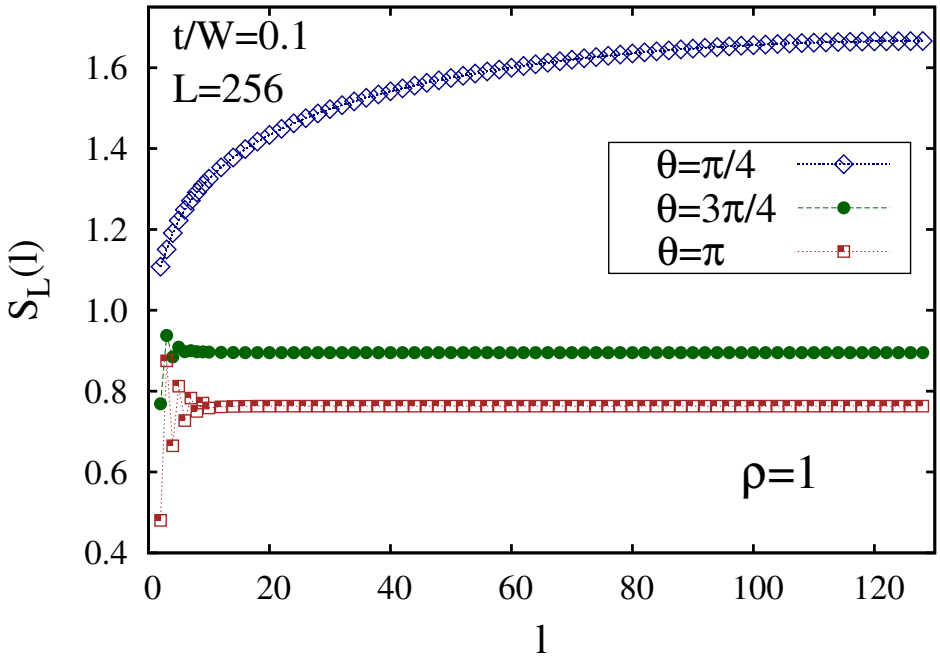

Figure 4-5: The von Neumann block entropy $S_L(l)$ as a function of l for a system with size $L = 256$, $\rho = 1$ and $t/W = 0.1$. Here we consider three different values of statistical angle: $\theta = \pi/4$, $\theta = 3\pi/4$, and $\theta = \pi$. The statistical angle drives a quantum phase transition.

density as a function of μ/W is the same for both values of the hopping. However, the Mott gap is obviously larger at $t/W = 0.4$ than at $t/W = 0.1$. This unusual result can be understood by taking into account that for generating a Mott insulator state with $\rho = 1$ under local three-body interactions, we need the interaction term to be important. For this, the quantum fluctuations must grow, which is caused by the hopping, and with the localization due to the statistics we obtain a larger interaction term, and finally the Mott gap increases with the hopping.

Previously, we showed that the behavior of the block von Neumann entropy allows us to distinguish between critical and noncritical ground states, for instance superfluid and Mott insulator states. With respect to the appearance of insulator states for larger values of the statistical angle, we want to verify the above results by means of the calculation of block entropy (3-5). We present the results in Fig. **4-5** for three different values of the angle, $\theta = \pi/4$, $\theta = 3\pi/4$, and $\theta = \pi$, setting the tunneling at $t/W = 0.1$, the global density at $\rho = 1$ and the lattice size at $L = 256$. For $\theta = \pi/4$, we observe that the entropy always increases until it diverges, which indicates that the system is in a superfluid phase. This is consistent with our previous results, in which a non-insulator region was found for this angle and this density (Fig. **4-2**). On the other hand, the above behavior of the block entropy changes for larger values of θ. Specifically, we observe that the block entropy increases very quickly exhibiting

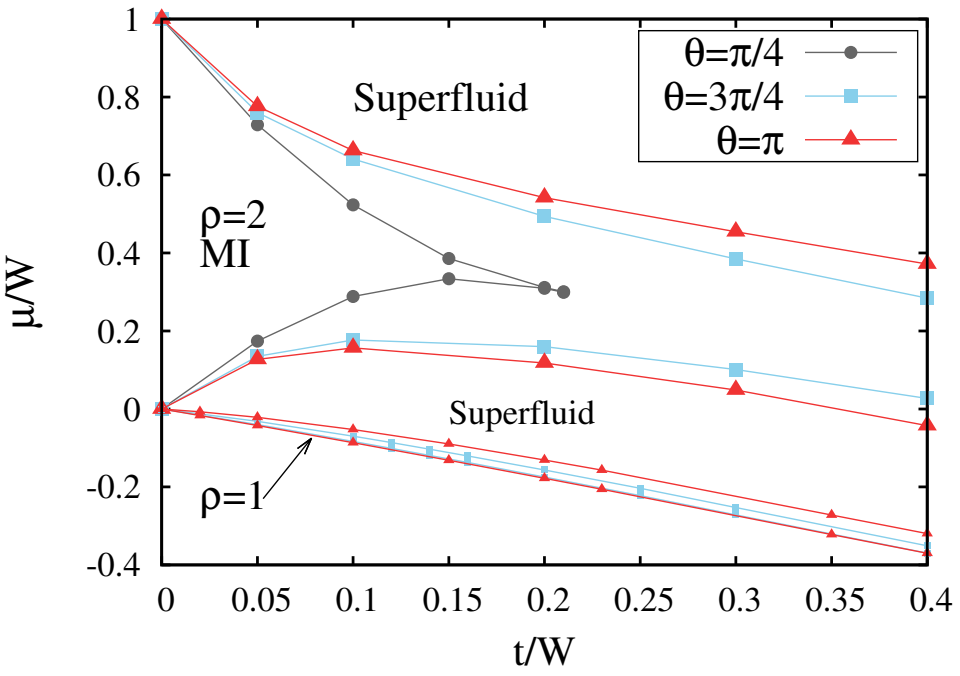

Figure 4-6: Phase diagram of the anyon-Hubbard model with local three-body interactions for $\theta = \pi/4$, $3\pi/4$, and π. Mott lobes and a superfluid phase were found, and their boundaries are marked by points that are extrapolations to the thermodynamic limit from DMRG data. The lines are visual guides.

an oscillator behavior for small values of the block size, but the range increases with the angle. We cannot explain this oscillator behavior, which is due to the statistics. After the short oscillation, the block entropy remains constant, showing that the system has a finite correlation length. Hence the ground state is a Mott insulator one. Another interesting fact is that the overall value of the von Neumann block entropy diminishes as the statistical angle grows, which indicates that the entanglement decreases. The above discussion allows us to conclude that the statistical angle θ drives a quantum phase transition from a superfluid to a Mott-insulator phase with $\rho = 1$.

We found that the statistics induce a Mott insulator region for larger values of the angle θ. This fact suggests that the phase diagram changes with the statistical angle, and we have to calculate this for statistical angles greater than $\theta = \pi/4$. In Fig. **4-6**, we also draw the results for $\theta = \pi/4$ shown in Fig. **4-2**, in order to compare them with the new results obtained, $\theta = 3\pi/4$ and $\theta = \pi$. We want to emphasize the absence of the $\rho = 1$ Mott lobe for $\theta = \pi/4$. At the atomic limit ($t/W = 0$), we observe that the Mott lobe regions are given by $\mu/W = \rho - 1$ regardless of the statistical angle; hence there is no Mott lobe with $\rho = 1$ at this limit. For the non-zero hopping parameter, we see that the Mott lobe with $\rho = 2$ decreases as t/W grows, a fact that is maintained for any angle; however, it is clear that

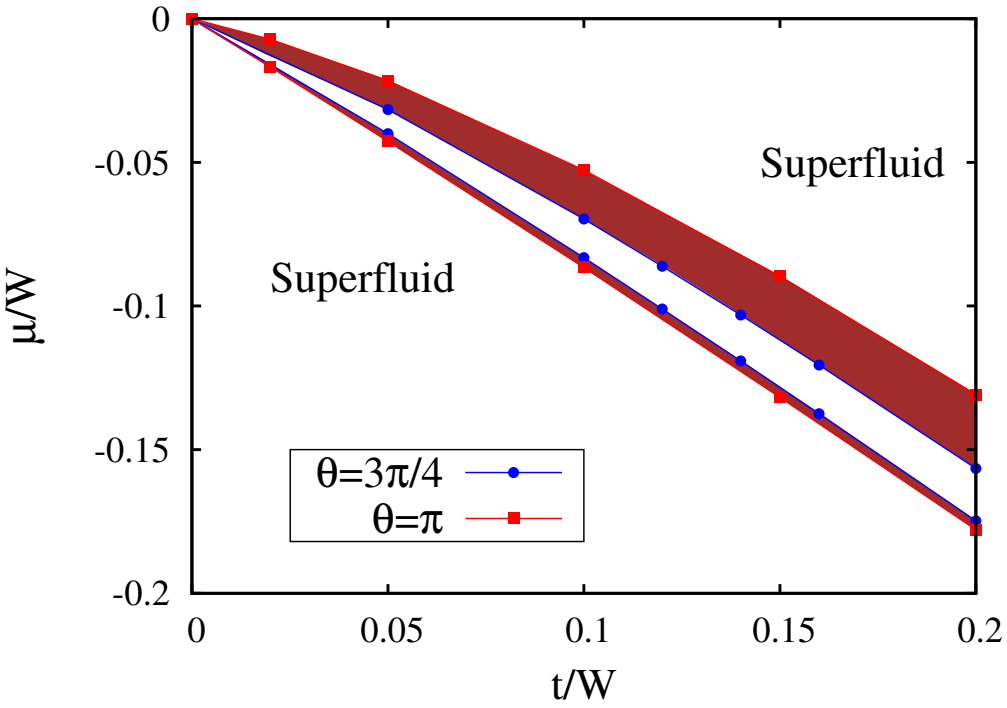

Figure 4-7: The $\rho = 1$ Mott lobe at the thermodynamic limit for a statistical angle $\theta = 3\pi/4$ and $\theta = \pi$. The lines are visual guides.

as the angle grows the statistics favor the localization of the particles, which is reflected in the increase of the Mott lobe area and the displacement of the critical point towards larger values. The phase diagram shows a much smaller $\rho = 2$ Mott lobe than the anyon chain with two-body interactions. Also, we obtained a re-entrant behavior for the $\rho = 2$ Mott lobe regardless of the statistical angle, i. e. for a fixed chemical potential value the ground state passes from a Mott insulator to a superfluid phase and then returns to the Mott insulator one. Note that this does not happen for the $\rho = 1$ Mott lobe (see Fig. 4-7). The emergence and evolution of the $\rho = 1$ Mott lobe as the hopping parameter increases is shown Fig. 4-7 for two different angles $\theta = 3\pi/4$ and $\theta = \pi$, where a zoom in has been made. From this it is clear that if the statistics increase, the localization grows. Note that for negative constant values of the chemical potential, the ground state is a superfluid with density lower than one. As the kinetic energy increases, it goes to a Mott insulator state with $\rho = 1$ and finally returns to a superfluid state, but with a density greater than one. From this figure, it is clear that the Mott lobe area increases with the hopping.

We showed that the statistical angle drives a quantum phase transition from a superfluid state to a Mott insulator one in the range of $\theta = \pi/4$-$3\pi/4$ for a fixed hopping parameter $t/W = 0.1$ and global density $\rho = 1$ (see Fig. 4-5). However a pending task is to explore the ground state phase diagram as a function of the statistical angle, which is shown in Fig. 4-8 for three different values of the hopping parameter, $t/W = 0.1$, 0.15, and 0.20. We obtain

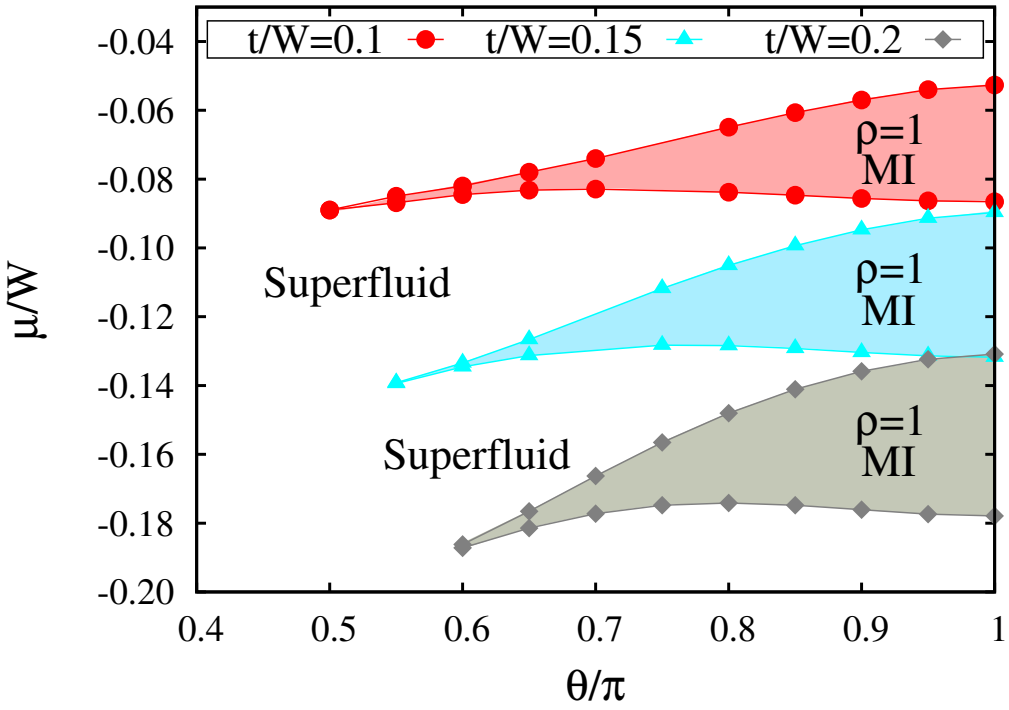

Figure 4-8: Phase diagram of the anyon-Hubbard model with local three-body interactions in the plane $(\mu/W, \theta/\pi)$. We consider three different hopping parameters $t/W = 0.1, 0.15$ and 0.2. The points are extrapolations to the thermodynamic limit from DMRG data and the lines are visual guides. MI means Mott insulator regions.

that there is a critical value of the angle at which the Mott insulator phase appears, and this critical value moves to greater values as the hopping grows. A reentrance phase transition was observed, since the hole excitation energy curve exhibits a maximum. Hence at some suitable constant chemical potential, the model displays a sequence of quantum phase transitions between the Mott insulator and the superfluid phases. In the sequence (from left to right), we have a change from a superfluid region with $\rho > 1$ to a Mott insulator one with $\rho = 1$ and then again to an superfluid region ($\rho < 1$), and finally the system remains in an insulator state. Finally, we note that for a fixed angle, the Mott lobe area increases with the tunneling. Note that the shape of the Mott lobes around the critical point is not elongated like others shown in Fig. **4-2** or others reported previously, which can indicate that this quantum phase transition is not of the Kosterlitz-Thouless type.

It is well known in the literature that using the gap vanishing point to determine the critical point related to a quantum phase transition gives us poor results and that some measures of the entanglement can help us in this task. Precisely, it has been shown that for models like the Bose-Hubbard one, the estimator based on the von Neumann block entropy $\Delta S_{LK}(L) = S_L(L/2) - S_{L/2}(L/4)$ proposed by Laüchli and Kollath leads to better results [17]. According

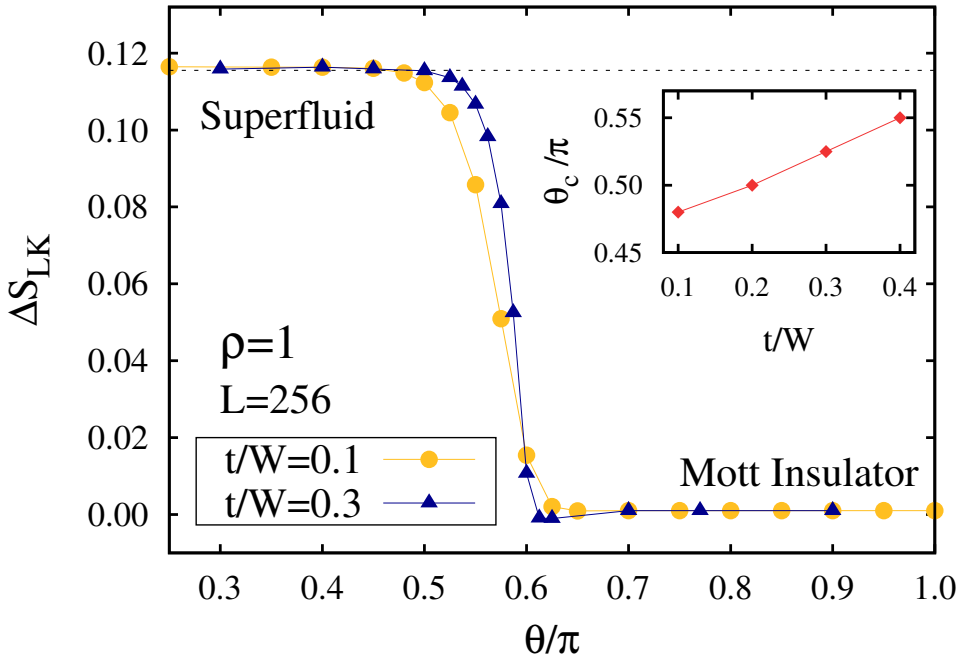

Figure 4-9: The estimator ΔS_{LK} as a function of angle θ for $t/W = 0.1$ and $t/W = 0.3$. Here we fixed L=256 and $\rho = 1$. The points are DMRG data and the lines are a visual guide. Inset: Evolution of the critical angle θ_c with the hopping parameter.

to above definition and the expression Eq. (3-5), we obtain:

$$\Delta S_{LK}(L) = \begin{cases} \frac{c}{6} ln[2], & \theta \leq \theta_c, \\ 0, & \theta > \theta_c, \end{cases} \tag{4-4}$$

θ_c being the critical angle.

In Fig. 4-9, the evolution of the estimator ΔS_{LK} with the statistical angle is shown for an anyon chain with $\rho = 1$, and $L = 256$. When $\theta = 0$, the ground state is a superfluid, because the $\rho = 1$ Mott insulator lobe does not exist for bosons under local three-body interactions. Therefore, the estimator will be equal to $ln(2)/6$, and it remains at this point for non-zero values of the statistical angle, indicating that there is a range of values of θ for which the ground state is a superfluid. However, from a given critical angle the estimator collapses to zero within a short range. After that, the estimator remains constant at zero, indicating that the ground state is now a Mott insulator one. Regardless of the hopping parameter, we see that the estimator clearly shows us the quantum phase transition from a superfluid to a Mott insulator state. Note that the superfluid region becomes greater and the shape of the curve becomes sharper as the hopping increases, although at the thermodynamic limit the shape of the curve will be a step function, according to the expression Eq. (4-4). The critical point corresponds to the greatest value of θ, for which the estimator is equal to $ln(2)/6$,

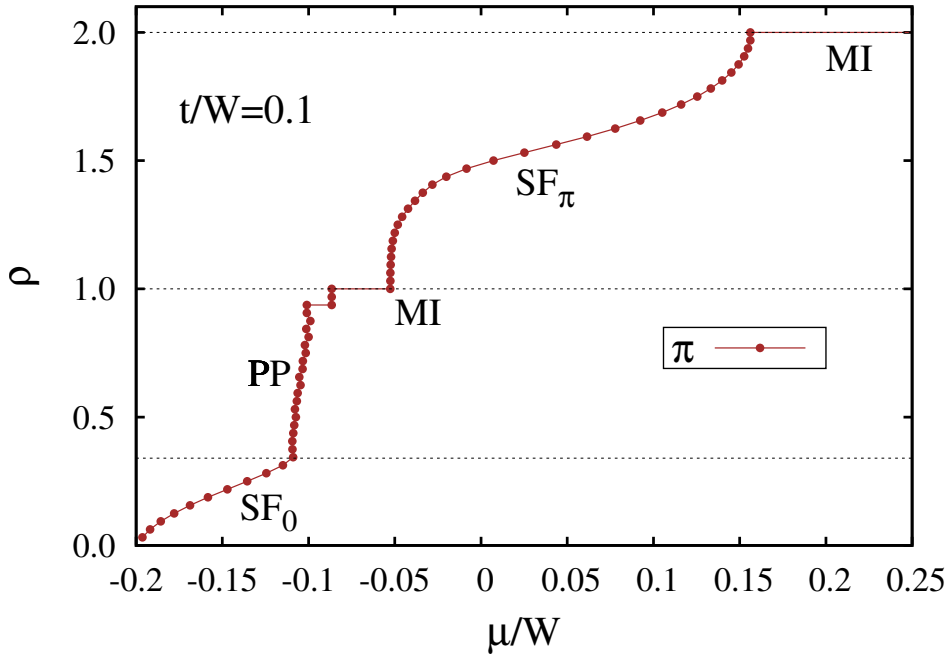

Figure 4-10: Density ρ vs chemical potential μ at the thermodynamic limit in the pseudo-fermion limit ($\theta = \pi$) up to density $\rho = 2$.

and we obtain that the position of the critical angle moves to greater values as the hopping grows (see inset of Fig. **4-9**).

Finally, to conclude our analysis on the model anyon-Hubbard with local three-body interactions we consider the study about pseudo-anyon Hubbard model ($\theta \to \pi$) [52]. They present the equation of state $\rho = \rho(\mu)$ for $\theta = \pi$ and small repulsive interaction. Several different phases and phase transitions may be observed [52]. We present in Fig. **4-10** the equation of state $\rho = \rho(\mu)$ for $\theta = \pi$ considering local three-body interactions. Using the reults of Zhang and co-workers [52], we compare qualitatively the two curves and we identified the type of quantum state for our system. Between $0 < \rho \lesssim 0.34$ the anyons would present a superfluid phase SF_0. After this value and up to a density closer 1, appears a jump in density giving rise a paired phase (PP). The Mott insulator can be indentified, as in the previous study, for the plateau at integer densities $\rho = 1$ and $\rho = 2$. The step-like behavior of the plateau with $\rho = 1$ may be associated with effect of finite system size and open boundary conditions [52]. For densities greater than 1, the system would present other superfluid phase SF_π. Finally, we have not strong indications of presence to paired phases between $1 < \rho < 2$, even so, this will be subject of a future study.

The ground state can be superfluid or Mott insulator, in accordance with our density matrix renormalization results for finite lattices. We build two phase diagrams, the chemical potential as a function of the statistical angle for a fixed hopping parameter and the che-

mical potential versus the hopping for a fixed anyonic angle. We found that an increase in the statistical angle generates a Mott insulator state with one anyon per site; therefore, a superfluid-Mott insulator transition driven by the statistics was observed. We expect that this quantum phase transition will be observed in the near future when recent proposals for creating an anyon system and obtaining a regime where the three-body interaction domain are realized.

Chapter 5

Conclusions and Perspectives

We have studied the properties of a collective of anyons loaded in an one-dimensional optical lattice at a zero temperature using the fractional version of the Jordan-Wigner transformation (an exact mapping between anyons and bosons). The study was performed by means of the density matrix renormalization group (DMRG), which has allowed us to obtain the phase diagram for different values of the statistical angle θ and densities $\rho = N/L$. The phase transition was studied using the block von Neumman entropy, and we were able to observe the superfluid to Mott insulator transition. In particular, we use the estimator proposed by Läuchli and Kollath to determine the critical points of the anyon-Hubbard model (it evidence, once again, the important relation beetwen the quantum phase transitions and the quantum information tools). It is important to note, that studies related to the most precise estimation of critical points have not been previously reported beyond the gap closing and that we consider the unexplored problem of delocalized anyons in a one-dimensional optical lattice under local three-body interactions (modified version of the anyon-Hubbard model). In the following, the main conclusions of the present thesis are summarized.

Anyon-Hubbard model with local two-body interactions

- ✓ We found that the anyon-Hubbard model exhibits two quantum phases: Mott insulator and superfluid. From results of the phase diagram for anyons with $\theta = \pi/4$ and the first three densities ($\rho = 1, 2$ and 3), we concluded that the density increase favors the appearance of the superfluid region, while the position of the critical point decreases. This result contradicts recently reported calculations of mean-field theory.

- ✓ For $\theta = \pi/4$ a reentrance phase transition was observed for $\rho = 1, 2, 3$. The reentrance transition is a sequence from Mott insulator to supefluid and back to Mott insulator at fixed value of chemical potential. This behavior is related with the maximium in the hole excitation energy.

- ✓ Related with the equation of state $\rho = \rho(\mu)$ for $\theta = \pi/4$ an important fact is that the slope is always greater than zero, i.e., the compressibility $\kappa = \partial\rho/\partial\mu > 0$, an argument

that is related to the absence of first-order transition. In this case, we conclude that the phase transitions for $\theta = \pi/4$ are of the second-order kind. However, the possibility of finding first-order transitions in the anyon-Hubbard model for larger values of θ and/or a fixed number of particles is an interesting open problem.

- ✓ The Mott lobes increase as a function of the statistical angle θ, this implies that the increase of the statistical angle leads to localization of the particles, a fact that can be relevant when many-body interactions between particles are considered, because, for instance, this can lead to obtaining Mott insulator phases for any density.

- ✓ Using the von Neumann block entropy and the estimator proposed by Lauchli and Kollath we calculated the evolution of the critical points with the density for $\theta = \pi/4$ and found an analytical expression $t_c/U = -0.037 + 0.45\rho^{-0.7}$.

- ✓ For $\rho = 1$ and $\rho = 2$, we showed that the gap closing can be fit to a Kosterlitz-Thouless expression and, taking into account that the central charge is $c = 0.97$, we argued that the anyon-Hubbard model with $\theta = \pi/4$ belongs to the same universality class as the Bose-Hubbard model.

Anyon-Hubbard model with local three-body interactions

- ✓ We found that the statistics drive a quantum phase transition from a superfluid phase to a Mott insulator one when the density is $\rho = 1$. As in the spinless and spinor boson cases, we obtain that for small statistical angles there is no Mott insulator region with density $\rho = 1$ when local three-body interactions are considered. However the above Mott insulator state emerges as the statistics grow, this fact being one of the main findings of this study, the absence of a Mott insulator state with one particle per site depends on the anyonic angle only. Which implies that the presence of fractional statistics favors the many-body interactions and increase in the quantum fluctuations, thus it is possible the appearance of insulator states with a very small number of particles and local three-body interactions.

- ✓ The expression $\mu/W = \rho - 1$ determines the width of the Mott lobes at the atomic limit, regardless of the statistics.

- ✓ The results indicate that the three-body interaction and the statistics favor the localization of particles and that a greater kinetic energy is required to delocalize the particles and generate superfluid states.

- ✓ The quantum phase transition of anyons under local three-body interactions was clearly identified by means of the von Neumann block entropy and the estimator proposed by Läuchli and Kollath. Using the latter to estimate the critical angles, we see that the hopping parameter moves the critical angles to greater values.

- ✓ In the pseudo-fermion limit ($\theta \to \pi$) the superfluid regions are modified, it appears superfluid phase SF_0, this superfluid is independent of the statistical angle; Other superfluid of type SF_π and regions with paired phases (PP). The characterization of these quantum states, using other quantity beyond of the calculation of chemical potential, it will be explore in a future study.

- ✓ Consider the determination of the critical points, in a more precise way, the phase diagrams reported will be useful for experimentalists in the setup for observing the phase transition in one-dimensional anyons. The study has the advantage that densities in a wide interval, along with different statistical angles, are considered. Furthermore, since the anyon model studied has correlated tunneling, our results are not restricted to the context of fractional statistics alone, but contribute to the study of models in which hopping depends on the local density, a field that has been the object of recent theoretical and experimental studies. The study of this correlated tunneling gives rise to nontrivial interaction and, being of great interest, has been applied in diverse contexts of Physics [71–73].

Perspectives - Other local interactions

It is important to mention other perspectives or an alternative proposal of this thesis. One important fact is that the local operators do not become modified when the Jordan-Wigner fractional transformation is used, it is possible to conceive of a modification of the local interaction because only the number operator is being involved. In the following, some alternative is present.

- Off-diagonal confinement [74]:

$$H = -\sum_{j}^{L-1} t_{kj} \left(b_j^\dagger b_{j+1} e^{i\theta n_j} + h.c. \right) + \frac{U}{2} \sum_{j}^{L} n_j(n_j - 1) + W \sum_{j}^{L} (j - L/2)^2 n_j, \quad (5\text{-}1)$$

with $t_{kj} = t(k + j + 1)(2L - i - j - 1)/L^2$

The aim will be to construct the phase diagrams for differents values of interaction and with the statistical angle as a free-parameter, which at this point could be relevant to compare to the bosonic case. In this sense, an interesting questions emerges: What are the quantum phases present in the system? And how do they modified the size, the borders and the critical points with the statistical parameter?. On the other hand, we could calculate the densities profile $< n_j >$ to determine the distribution of particles on a lattice as a dependence of harmonic trapping potential.

Perspectives - DMRG-t

Other interesting problem is the extension of the density matrix renormalization group incorporating the real-time evolution [75]. It is relevant in the context of the experimental setups which is possible to study of the time evolution of quantum systems and the posibility of understand the time evolution of observables and/or the evolution of correlation functions in quenched systems. The method have been successful in the transport in nano-structures [76], spectral properties in one-dimension [75] and among others, the finite-temperature DMRG [77, 78].

Studies related to this field for anyons in one-dimensional lattice have not been previously reported. In this case, we are interested in the time evolution study of the local correlation. In particular, the evolution of expected value of the number operator and its dependence on the anyonic statistics. Also, considering the relation beetwen entanglement and the critical behaviors and the determination of the quantum phase, it is relevant to understand the dynamical properties of entanglement. This is the main aim of these perspectives.

We describe an extension to the density matrix renormalization group (DMRG) method incorporating real-time evolution. The study of time-evolution of a quantum state is an interesting problem in the context of the transport problem, dynamical correlation functions and systems driven out of equilibrium, quenches, among others [75]. We write the time-dependent Schrödinger equation, $|\psi(t)\rangle$ under action of a Hamiltoanian $\mathcal{H}$:

$$i\frac{\partial}{\partial t}|\psi(t)\rangle = \mathcal{H}|\psi(t)\rangle\,, \tag{5-2}$$

where we have used $\hbar = 1$. The time-evolution operator apply on particular Hamiltonian is given by $U(t) = e^{-i\mathcal{H}t}$, by mean of expansion in the eigenbasis to the Hamiltonian leading to $|\psi(0)\rangle = \sum_n C_n|\psi_n\rangle$ (with time-independent coefficients c_n), we have the time-evolution as

$$|\psi(t)\rangle = U(t)|\psi(0)\rangle = \sum_n C_n e^{-iE_n t}|\psi_n\rangle\,. \tag{5-3}$$

The t-DMRG was developed by Daley *et al.* and White and Feiguin [75, 79], for systems with nearest neighbor interactions (coupling sites j and $j+1$), then the time evolution operator is $e^{-i\mathcal{H}\tau}$, with $\tau = \Delta t$. They adapt the Suzuki-Trotter decomposition to match the DMRG finite-system sweeps. They decompose the time propagator as [75]:

$$e^{-i\mathcal{H}\Delta t} \approx e^{-iH_1\Delta t/2}e^{-iH_2\Delta t/2}\ldots e^{-iH_2\Delta t/2}e^{-iH_1\Delta t/2}. \tag{5-4}$$

The aim is then to apply $e^{-iH_1\Delta t/2}$ at DMRG step 1, then $e^{-iH_2\Delta t/2}$ at the step 2, etc., forming the left-to- right sweep, then reverse, applying all the reverse order terms in the right-to-left sweep. Is important to note that before of applied the time evolution operator,

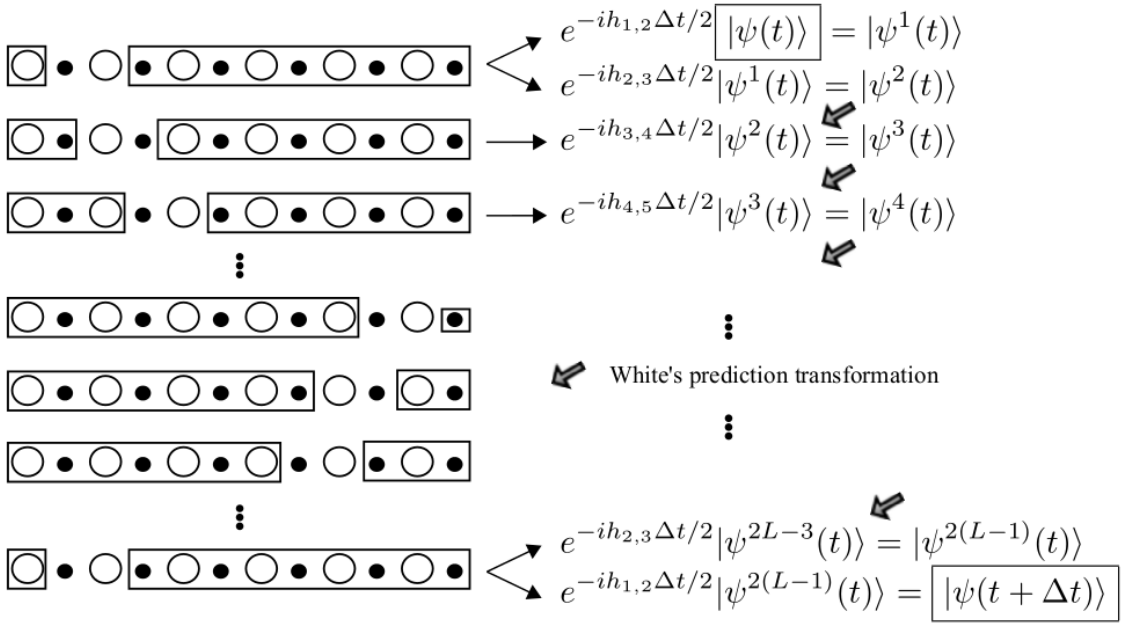

Figure 5-1: Schematic representation of the adaptive t-DMRG algorithm.

the ground state is to found by mean the use of standard DMRG. This procedure requires one to use the step-to-step wave function transformation first developed to provide a good guess for the Lanczos or Davidson diagonalization [75].

A schematic representation of the adaptive t-DMRG algoritm is shown in Fig. **5-1**. Is possible to see the transformation of state $\left|\psi^k t\right\rangle$ for the action of the operator $e^{-ih_{k,k+1}\Delta t/2}$ with $H = \sum_i h_{i,i+1}$, in one DMRG sweep.

Appendix A

Density Matrix Renormalization Group (DMRG) Method

The density matrix renormalization group (DMRG) method was developed by S. White in 1992 [27], in order to solve the numerical limitations of the standar renormalization group of Wilson [80]. He shows the power of this numerical tool in the study of interacting systems in low dimensions and has become a powerful numerical method that can be applied to strongly-correlated fermionic and bosonic systems. Its field of applicability has now been extended beyond condensed matter, and it is successfully used in statistical mechanics and high-energy physics. The DMRG allows for a systematic truncation of the Hilbert space by keeping the most probable states (highest probability in the system) that describe a wave function [28].

We consider the renormalization gruop for one-dimensional models, the first iteration begin when we divided the system in two indentical blocks of finite size. Each block B corresponds to a Hamiltonian H_B, we replace the site 1 by the block formed by sites 1 and 2 and we obtained the m lowest states $|u_\alpha\rangle$, the next step is write the new Hamiltonian by mean of the transformation $H'_B = OH_{BB}O^\dagger$, with $O_{i_1 i_2} = u_{i_1 i_2}$. The process is repeated until we have the number of sites desired in the lattice.

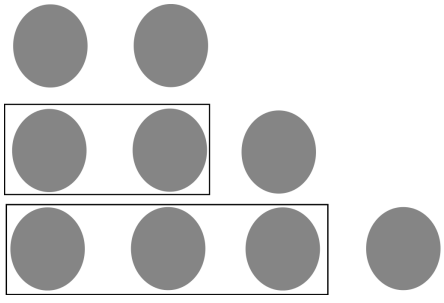

Figure A-1: Numerical renormalization group.

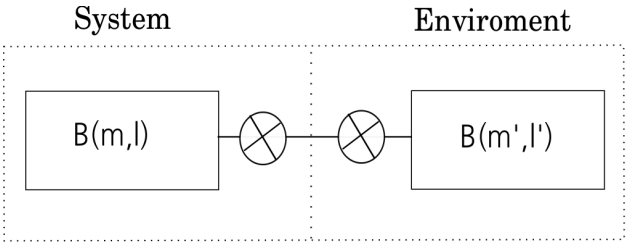

Figure A-2: Configuration of blocks used in DMRG

When is considered the boundary conditions, it is possible that the two blocks are disconnected, which implies the eigenstates posses behaviors not expected in the frontier of lattice.

For the DMRG method we consider the system divide it in two parts, the first is called, *system* and the second is called, *enviroment* block, which forms a superblock (Fig. **A-2**). The DMRG proposed a truncation procedure of the density matrix in order to choose the most important states [27, 81], keeping the m most probable eigenstates of the reduced density matrix of the enlarged block with respect to the superblock gives its most accurate representation, in a m-dimensional Hilbert space.

We are interested in the ground state of superblock, which contains the information of both the system and the environment, and is given by

$$|\psi_0\rangle = \sum_{ij} \psi_{ij} |i\rangle |j\rangle , \tag{A-1}$$

when $|i\rangle$ and $|j\rangle$ are the orthonormal bases of system and environment respectively. ψ_{ij} represent the probability amplitude of finding the system and the environment in the i and j state. We retained the most probable states of the system block for some $|\psi\rangle$, we consider the environment as a statistical bath and the reduced density matrix for the system defined by

$$\rho_{ii'} = \sum_{j} \psi^*_{ij}\psi_{i'j}, \tag{A-2}$$

Due to normalization we have that $Tr(\rho) = 1$. If we want to obtain the expected value of an observable A of the system and also we know that the operator only acts on block's system, we use the next relation

$$\langle A\rangle = \sum_{ii'} A_{ii'}\rho_{i'i} = Tr(\rho A) \tag{A-3}$$

If we change the base of the density matrix by means of diagonalization, considering the eigenvectors of $\rho |\alpha\rangle$ and their eigenvalues ω_α as

$$\langle A\rangle = \sum_{\alpha} w_\alpha \langle u^\alpha| A |u^\alpha\rangle \tag{A-4}$$

In this case, is possible to neglected states $|\alpha\rangle$ for which $w_\alpha \approx 0$ without incurring in an appreciable error given rise to a renomarmalization process.

We can write the error as

$$\epsilon_\rho = 1 - \sum_{\alpha}^{m} w_\alpha, \tag{A-5}$$

which is minimum when the larger values of ω_α are taken [27, 81]. There are two types of DMRG algorithms: the infinite and finite methods.

A.0.1. Infinite System Algorithm

In this method we begin the process with a determined size of the system block, and in each step a site is added to it. The environment block is chosen as a reflection of the system. The Fig. **A-3** shows the configuration of the system. In the table I is shown the step by step of the algorithm.

Table I Infinite system algorithm for a one-dimensional quantum system [27, 81].

1. Begin with four blocks, each one with a single site. Define the matrices that represent the Hamiltonians of each block and other relevant operators.
2. Build the Hamiltonian of the superblock by a direct products of operators.
3. Using the Lanczos method or other analogous method for the diagonalization of Hamiltonian to found the target states, $|\psi_0\rangle$.
4. Build the reduced density matrix ρ for the ground state.
5. Diagonalize the density matrix to obtain its eigenvalues and its eigenvectors. Retained only the m eigenvectors u_{ij}^{α} corresponding to the m largest eigenvalues ω_α.
6. Make the matricial representations of the system's operators the two sites that form it, by means of the appropriate direct products.
7. Build a new operator O, the colums of O contents the m selected eigenvectors of ρ.
8. Using the operation, $\tilde{H} = O^\dagger H O$ and $\tilde{A} = O^\dagger A O$, to transform the Hamiltonian and operators respectively
9. Keep old block 1 and replace it with the new one.
10. Keep old block 4 and replace it with the reflection of the new block.
11. Go to step 2.

A.0.2. Finite System Algorithm

The infinite system algorithm is the best option when we desire the different quantities at the thermodynamic limit ($N, L \to \infty$). This algorithm is employed when the size of the system desired in the infinite system algorithm is reaches. The Fig. **A-4** shows the configuration of

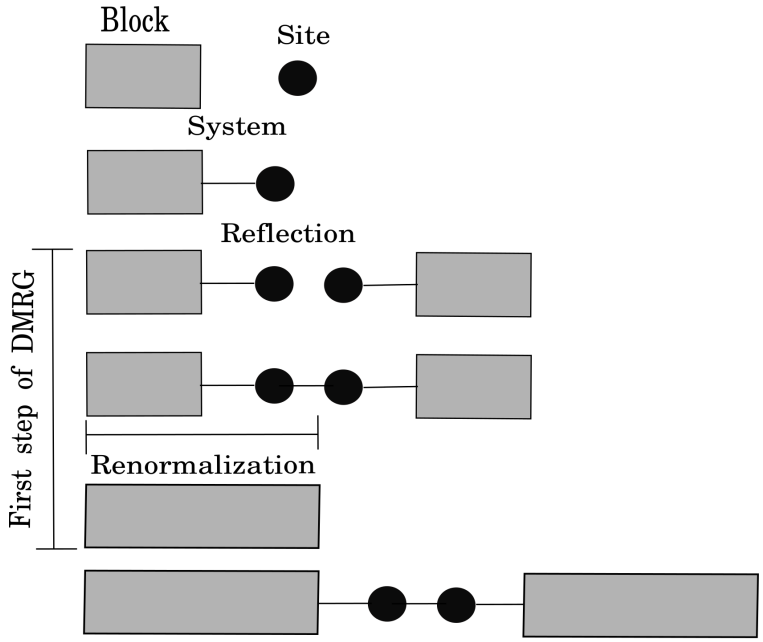

Figure A-3: Schematic procedure for the infinite-system DMRG algorithm is shown.

the system. In the table II is shown the step by step of the algorithm.

Tabla II Finite System Algorithm [27, 81].

1. Build a superblock of lenght L using the infinite system algorithm (Table I); l corresponds to the size of the first space of the system, denoted as $B(l)$.
2. Make $l = L/2$ and use $B(l)$ as space 1 and the reflection $B(L-1-l-2)$ as space 4.
3. Use the steps 2 to 9 of the infinite algorithm (Table I).
4. Replace space 4 with the reflection of $B(L-(l+1)-2)$, using the information saved during the infinite system method.
5. If $l < L-3$, increase the size of the system, making $l = l+1$.
6. Repeat steps 3-5 until $l = L-3$. This is the left-to-right sweep.
7. Take the 4 initial blocks, the first three consisting on one single site and the fourth being the reflection of $B(L-3)$, found in the previous step. Make $l = 1$.
8. Use the steps 2 to 9 of the infinite algorithm (Table I).
9. Keep the new block $B(l+1)$ for the initial space.
10. Make the reflection $B(L-(l+1)-2)$ and supersede the space 4.
11. Make $l = l+1$, and repeat steps 8-10 until $l = L-3$. This is the right-to-left sweep. Once the equality is obtained, go back to step 7 to repeat the sweep.
12. Repeat the process and finish the process at a symmetric configuration.

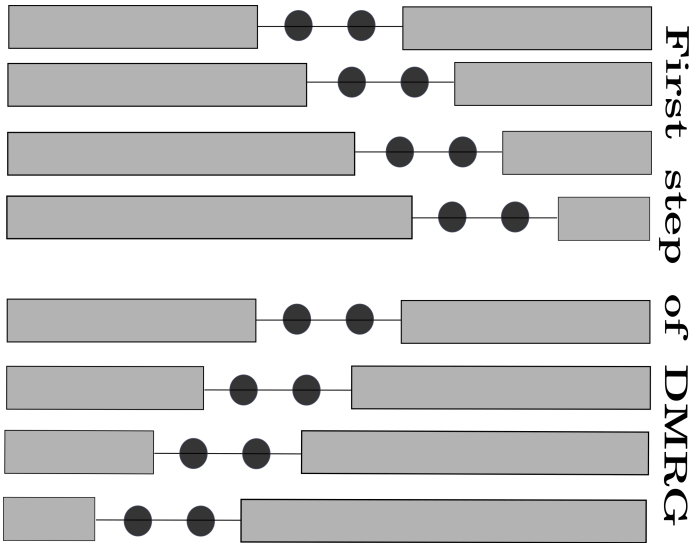

Figure A-4: Schematic procedure for the DMRG algorithm. A complete finite-system DMRG sweep is depicted

A.1. Dynamical Block State Selection (DBSS) Method

This method is a protocol based on a fixed truncation error of the subsystem's reduced density matrix instead of using a fixed number of preserved states in the DMRG sweeps [56]. In the standar DMRG the number of states kept are fixed for each sweep. However, other interesting way is established the tolerant value of the truncation error as a initial parameter of routine. In this case, the number of states retained m are dynamically to found with the variant in the code by the expression,

$$\sum_{j=1}^{m} \omega_j = 1 - \epsilon < 1 - X_{error}, \tag{A-6}$$

where X_{error} is the truncation error. Thus, we make control over the truncation error with the aim to choose the correct number of eigenstates of the density matrix, which implies a significant efficiency and the time involved is optimized. This modification is related with the fact that the number of states requiered is different for each set of parameter. For the anyon-Hubbard model the number of maintained states increases as the angle tends to $\theta = \pi$.

Bibliography

[1] T. Keilmann, S. Lanzmich, I. McCulloch, and M. Roncaglia *Nat. Commun.*, vol. 2, p. 361, 2011. x, xiv, xiv, xiv, xiv, 3, 4, 5, 6, 8, 9, 10, 11, 12, 14, 15, 19, 20, 22, 23, 32, 35, 37, 38

[2] S. Greschner and L. Santos *Phys. Rev. Lett.*, vol. 115, p. 053002, 2015. xiv, 4, 14, 16, 19

[3] C. Sträter, S. C. Srivastava, and A. Eckardt *Phys. Rev. Lett.*, vol. 117, no. 20, p. 205303, 2016. xiv, 14, 16, 17, 18

[4] I. Danshita and A. Polkovnikov *Phys. Rev. A*, vol. 84, p. 063637, 2011. xv, 30, 31

[5] J. M. Leinaas and J. Myrheim *Il Nuovo Cimento B*, vol. 37, pp. 1–23, 1977. 1, 7

[6] F. Wilckzek *Phys. Rev. Lett.*, vol. 49, p. 957, 1982. 1, 2, 7

[7] A. Kitaev *Ann. Phys.*, vol. 303, p. 2, 2003. 1, 2, 7

[8] J. K. Pachos. Cambridge University Press, 2012. 2

[9] D. C. Tsui, H. Stormer, and J. Gossard *Phys. Rev. Lett.*, vol. 48, p. 1559, 1982. 2, 7

[10] R. B. Laughlin *Phys. Rev. Lett.*, vol. 50, p. 1395, 1983. 2, 7

[11] F. Haldane *Phys. Rev. Lett.*, vol. 67, p. 937, 1991. 2, 7

[12] P. Jordan and E. P. Wigner *Z. Phys.*, vol. 47, pp. 631–651, 1928. 3

[13] Y. Hao, Y. Zhang, and S. Chen *Phys. Rev. A*, vol. 79, p. 043633, 2009. 4, 8

[14] Y. Hao and S. Chen *Phys. Rev. A*, vol. 86, p. 043631, 2012. 4, 8

[15] J. Silva-Valencia and A. M. C. Souza *Phys. Rev. A*, vol. 84, p. 065601, 2011. 5

[16] A. O. L. Amico, R. Fazio, and V. vedral *Rev. Mod. Phys.*, vol. 80, p. 517, 2008. 5, 25

[17] A. M. Läuchli and C. Kollath *J. Stat. Mech*, p. P05018, 2008. 5, 25, 27, 32, 44

[18] J. Silva-Valencia and A. M. C. Souza *Eur. Phys. J. B*, vol. 85, p. 161, 2012. 5

[19] R. Islam, R. Ma, P. M. Preiss, M. E. Tai, A. Lukin, M. Rispoli, and M. Greiner *Nature*, vol. 528, no. 7580, pp. 77–83, 2015. 5

[20] A. J. Daley and J. Simon *Phys. Rev. A*, vol. 89, no. 5, p. 053619, 2014. 5, 6, 34

[21] I. Bloch, J. Dalibard, and W. Zwerger *Rev. Mod. Phys.*, vol. 80, pp. 885–964, Jul 2008. 6, 34

[22] D. Jaksch and P. Zoller *Ann. of phys.*, vol. 315, no. 1, pp. 52–79, 2005. 6, 34

[23] H. Büchler, A. Micheli, and P. Zoller *Nat. Phys.*, vol. 3, no. 10, pp. 726–731, 2007. 6, 34

[24] P. Johnson, E. Tiesinga, J. Porto, and C. Williams *N. J. of Phys.*, vol. 11, no. 9, p. 093022, 2009. 6, 34

[25] S. Will, T. Best, U. Schneider, L. Hackermüller, D.-S. Lühmann, and I. Bloch *Nature*, vol. 465, no. 7295, pp. 197–201, 2010. 6, 34

[26] J. Arcila-Forero, R. Franco, and J. Silva-Valencia *Phys. Rev. A*, vol. 94, p. 013611, Jul 2016. 6, 9, 37, 38

[27] S. R. White *Phys. Rev. Lett.*, vol. 69, p. 2863, 1992. 6, 53, 54, 55, 56

[28] K. A. Hallberg *Adv. in Phys.*, vol. 55, no. 5-6, pp. 477–526, 2006. 6, 53

[29] A. L. Fetter, C. Hanna, and R. Laughlin *Phys. Rev. B*, vol. 39, p. 9679, 1989. 7

[30] Y. H. Chen, F. Wilczek, E. Witten, and B. Halperin *Int. Jour. Mod. Phys. B*, vol. 3, p. 1001, 1989. 7

[31] B. I. Halperin *Phys. Rev. Lett.*, vol. 52, p. 1583, 1984. 7

[32] F. E. Camino, W. Zhou, and V. J. Goldman *Phys. Rev. B*, vol. 72, p. 075342, 2005. 7

[33] C. Nayak, S. H. Simon, A. Stern, M. Freedman, and S. D. Sarms *Rev. Mod, Physics.*, vol. 80, p. 1083, 2008. 7

[34] J. Alicea, Y. Oreg, G. Rafael, F. von Oppen, and M. P. A. Fisher *Nat. Phys.*, vol. 7, p. 412, 2011. 7

[35] A. Kundu *Phys. Rev Lett.*, vol. 83, p. 1275, 1999. 7

[36] M. Batchelor, X.-W. Guan, and N. Oelkers *Phys. Rev Lett.*, vol. 96, p. 210402, 2006. 7

[37] M. D. Girardeau *Phys. Rev. Lett.*, vol. 97, p. 100402, 2006. 7

[38] P. Calabrese and M. Mintchev *Phys. Rev. B*, vol. 75, p. 233104, 2007. 8

[39] C. Vitoriano *Phys. Rev. Lett.*, vol. 102, p. 146404, 2009. 8

[40] N. Zinner *Phys. Rev. A*, vol. 92, no. 6, p. 063634, 2015. 8

[41] O. I. Pâţu *J. Stat. Mech.*, no. 1, p. P01004, 2015. 8

[42] B. Paredes, P. Fedichev, J. I. Cirac, and P. Zoller *Phys. Rev. Lett.*, vol. 87, p. 010402, 2001. 8

[43] X. Xie, S. He, and S. D. Sarma *Physical review letters*, vol. 66, no. 3, p. 389, 1991. 8

[44] L.-M. Duan, E. Demler, and M. D. Lukin *Phys. Rev. Lett.*, vol. 91, p. 090402, 2003. 8

[45] L. Jiang, G. K. Brennen, A. V. Gorshkov, K. Hammerer, M. Hafezi, E. Demler, M. D. Lukin, and P. Zoller *Nat. Phys.*, vol. 4, p. 482, 2008. 8

[46] M. Aguado, G. K. Brennen, F. Verstraete, and J. I. Cirac *Phys. Rev. Lett.*, vol. 101, p. 260501, 2008. 8

[47] S. Longhi and G. D. Valle *Opt. Lett.*, vol. 37, p. 11, 2012. 8

[48] Y. Zhang, G. J. Sreejith, and J. K. Jain *Phys. Rev. B*, vol. 92, p. 075116, 2015. 8

[49] G. Tang, S. Eggert, and A. Pelster *N. Jour. of Phy.*, vol. 17, no. 12, p. 123016, 2015. 9

[50] W. Zhang, E. Fan, T. C. Scott, and Y. Zhang *arXiv:1511.01712*, 2015. 9

[51] G. Marmorini, M. Pepe, and P. Calabrese *J. Stat. Mech: Theor. Exp.*, vol. 2016, no. 7, p. 073106, 2016. 9

[52] W. Zhang, S. Greschner, E. Fan, T. C. Scott, and Y. Zhang *arXiv preprint arXiv:1609.02594*, 2016. 9, 19, 46

[53] F. Lange, S. Ejima, and H. Fehske *arXiv preprint arXiv:1612.00605*, 2016. 9, 19

[54] F. Lange, S. Ejima, and H. Fehske *ArXiv*, vol. 1704.07197v1, 2017. 9

[55] J. Carrasquilla, S. R. Manmana, and M. Rigol *Phys. Rev. A*, vol. 87, p. 043606, 2013. 20, 35

[56] O. Legeza, J. Roder, and B. A. Hess *Phys. Rev. B*, vol. 67, p. 125114, 2003. 20, 35, 57

[57] C. Weeks, G. Rosenberg, B. Seradjeh, and M. Franz *Nat. Phy.*, vol. 3, pp. 796–801, 2007. 20

[58] G. Batrouni and R. Scalettar *Phys. Rev. Lett.*, vol. 84, no. 7, p. 1599, 2000. 22

[59] L. d. F. de Parny, F. Hébert, V. Rousseau, and G. Batrouni *Phys. Rev. B*, vol. 88, no. 10, p. 104509, 2013. 22

[60] G. Batrouni, V. Rousseau, and R. Scalettar *Phys. Rev. Lett.*, vol. 102, no. 14, p. 140402, 2009. 22

[61] S. Ejima, H. Fehske, and F. Gebhard *Europhys. Lett.*, vol. 93, p. 30002, 2011. 24, 25, 28

[62] T. D. Kühner, S. R. White, and H. Monien *Phys. Rev. B*, vol. 61, p. 12474, 2000. 24, 25

[63] M. Pino, J. Prior, A. M. Somoza, D. Jaksch, and S. R.Clark *Phys. Rev. A*, vol. 86(2), p. 023631, 2012. 24

[64] T. D. Kühner and H. Monien *Phys. Rev. B*, vol. 58, p. R14741(R), 1998. 24

[65] S. Rachel, N. Laflorencie, H. F. Song, and K. L. Hur *Phys. Rev. Lett.*, vol. 108, p. 116401, 2012. 25

[66] S. Ejima, H. Fehske, F. Gebhard, K. zu Munster, M. Knap, E. Arrigoni, and W. von der Linden *Phys. Rev. A*, vol. 85, p. 053644, 2012. 25

[67] P. Calabrese and J. Cardy *J. Stat. Mech: Theor. Exp.*, vol. 06, p. P06002, 2004. 26

[68] J. Xavier and F. C. Alcaraz *Phys. Rev. B*, vol. 84, no. 9, p. 094410, 2011. 27

[69] J. M. Kosterlitz and D. J. Thouless *J. of Phys. C*, vol. 6, p. 1181, 1973. 29

[70] C. Avila, R. Franco, A. M. C. Souza, M. Figueira, and J. Silva-Valencia *Phys. Lett. A*, vol. 378, no. 44, pp. 3233–3236, 2014. 38

[71] L. Cardarelli, S. Greschner, and L. Santos *Phys. Rev. A*, vol. 94, no. 2, p. 023615, 2016. 50

[72] S. Greschner, G. Sun, D. Poletti, and L. Santos *Phys. Rev. Lett.*, vol. 113, no. 21, p. 215303, 2014. 50

[73] M. Di Liberto, C. Creffield, G. Japaridze, and C. M. Smith *Phys. Rev. A*, vol. 89, no. 1, p. 013624, 2014. 50

[74] V. Rousseau, K. Hettiarachchilage, M. Jarrell, J. Moreno, and D. Sheehy *Phys. Rev. A*, vol. 82, no. 6, p. 063631, 2010. 50

[75] S. R. White and A. E. Feiguin *Phys. Rev. Lett.*, vol. 93, no. 7, p. 076401, 2004. 51, 52

[76] D. Gobert, C. Kollath, U. Schollwöck, and G. Schütz *Phys. Rev. E*, vol. 71, no. 3, p. 036102, 2005. 51

[77] S. Sota and T. Tohyama *Phys. Rev. B*, vol. 78, no. 11, p. 113101, 2008. 51

[78] S. R. White *Phys. Rev. Lett.*, vol. 102, no. 19, p. 190601, 2009. 51

[79] A. J. Daley *J. Stat. Mech: Theor. Exp.*, vol. 04, p. P04005, 2004. 51

[80] K. G. Wilson *Rev. Mod. Phys.*, vol. 47, p. 773, 1975. 53

[81] S. R. White *Phys. Rev. B*, vol. 48, p. 10345, 1993. 54, 55, 56